Journal Pre-proofs

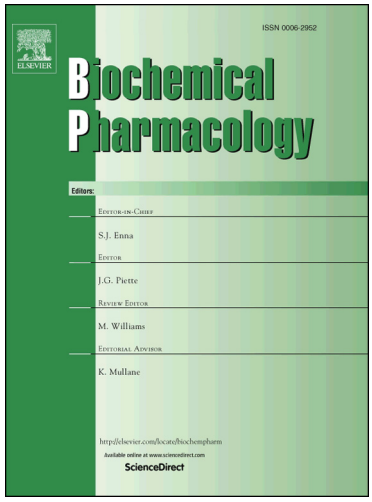

Olean–28,13b–olide 2 plays a role in cisplatin–mediated apoptosis and reverses cisplatin resistance in human lung cancer through multiple signaling pathways

Bin Zhu, Caiping Ren, Ke Du, Hecheng Zhu, Yong Ai, Fenghua Kang, Yi Luo, Weidong Liu, Lei Wang, Xu Yang, Xingjun Jiang, Yihua Zhang

PII: S0006-2952(19)30341-7
DOI: https://doi.org/10.1016/j.bcp.2019.113642
Reference: BCP 113642

To appear in: *Biochemical Pharmacology*

Received Date: 25 July 2019
Accepted Date: 16 September 2019

Please cite this article as: B. Zhu, C. Ren, K. Du, H. Zhu, Y. Ai, F. Kang, Y. Luo, W. Liu, L. Wang, X. Yang, X. Jiang, Y. Zhang, Olean–28,13b–olide 2 plays a role in cisplatin–mediated apoptosis and reverses cisplatin resistance in human lung cancer through multiple signaling pathways, *Biochemical Pharmacology* (2019), doi: https://doi.org/10.1016/j.bcp.2019.113642

Olean-28,13b-olide 2 plays a role in cisplatin-mediated apoptosis and reverses cisplatin resistance in human lung cancer through multiple signaling pathways

BIN ZHU[1,4], CAIPING REN[1,4], KE DU[2], HECHENG ZHU[4], YONG AI[3], FENGHUA KANG[3], YI LUO[3], WEIDONG LIU[1,4], LEI WANG[1,4], XU YANG[4], XINGJUN JIANG[1] and YIHUA ZHANG[3]

[1]Cancer Research Institute, Department of Neurosurgery, School of Basic Medical Science, Xiangya Hospital, Central South University, Changsha, Hunan 410008; [2]Hunan University of Chinese Medicine, Changsha, Hunan 410208; [3]State Key Laboratory of Natural Medicines, China Pharmaceutical University, Nanjing, Jiangsu 210009; [4]Changsha Kexin Cancer Hospital, Changsha, Hunan 410205

Correspondence to: Professor Caiping Ren, Cancer Research Institute, School of Basic Medical Science, Xiangya Hospital, Central South University, 87 Xiangya Road, Changsha, Hunan 410008, P.R. China

E-mail: rencaiping@csu.edu.cn

Professor Yihua Zhang, State Key Laboratory of Natural Medicines, China Pharmaceutical University, 24 Tongjiaxiang, Nanjing, Jiangsu 210009, P.R. China

E-mail: yhz@cpu.edu.cn

Key words: olean-28,13b-olide 2, thioredoxin reductase, P-glycoprotein, apoptosis, non-small cell lung cancer, multi-targeted agent

Running title: ZHU *et al*: ROLE OF OLO-2 IN CISPLATIN-MEDIATED APOPTOSIS AND CISPLATIN RESISTANCE IN LUNG CANCER

Abstract. Lung cancer, similar to other chronic diseases, occurs due to perturbations in multiple signaling pathways. Mono-targeted therapies are not ideal since they are not likely to be effective for the treatment and prevention of lung cancer, and are often associated with drug resistance. Therefore, the development of multi-targeted agents is required for novel lung cancer therapies. Thioredoxin reductase (TrxR or TXNRD1)

is a pivotal component of the thioredoxin (Trx) system. Various types of tumor cells are able to overexpress TrxR/Trx proteins in order to maintain tumor survival, and this

overexpression has been shown to be associated with clinical outcomes, including irradiation and drug resistance. Emerging evidence has indicated that oleanolic acid (OA) and its derivatives exhibit potent anticancer activity, and are able to overcome drug resistance in cancer cell lines. In the present study, it was demonstrated that a

novel synthesized OA family compound, olean-28,13b-olide 2 (OLO-2), synergistically enhanced cisplatin (CDDP)-mediated apoptosis, led to the activation of caspase-3 and the generation of reactive oxygen species (ROS), induced DNA damage, and inhibited the activation of the extracellular-signal-regulated kinase (ERK), signal transducer and activator of transcription 3 (STAT3), AKT and nuclear factor-κB (NF-κB) pathways in human multidrug-resistant A549/CDDP lung adenocarcinoma cells. Subsequent analyses revealed that OLO-2 inhibited P-glycoprotein (P-gp or ABCB1) and TrxR by reducing their expression at the protein and mRNA levels, and by suppressing P-gp ATPase and TrxR activities. Further biological evaluation indicated that OLO-2 significantly reduced Trx and excision repair cross-complementary1 (ERCC1) protein expression and significantly inhibited the proliferation of drug-sensitive (A549) and multidrug-resistant (A549/CDDP) non-small cell lung cancer (NSCLC) cells, but had no effect on non-tumor lung epithelial-like cells. In addition, the present study demonstrated, for the first time, to the best of our knowledge, that overexpressing or knocking down TrxR in NSCLC cells enhanced or attenuated, respectively, the resistance of NSCLC cells against CDDP, which indicated that TrxR plays an important role in CDDP resistance and functions as a protector of NSCLC against chemotherapeutic drugs. OLO-2 treatment also exhibited up to 4.6-fold selectivity against human lung adenocarcinoma cells. Taken together, the results of the present study shed light on the drug resistance-reversing effects of OLO-2 in lung cancer cells.

1. Introduction

Lung cancer is one of the leading causes of cancer-associated mortality worldwide, accounting for as many as 1.3 million deaths per year [1, 2]. Non-small cell lung cancer (NSCLC) accounts for ~85% of all cases of lung cancer [3], and lung adenocarcinoma has become the major pathological type of NSCLC [4]. Although chemotherapy is currently the standard treatment for advanced NSCLC, the majority of patients develop cross-resistance to various chemotherapeutic drugs [a phenomenon termed 'multiple drug resistance' or multidrug resistance (MDR)] [5]. P-glycoprotein (P-gp or ABCB1), a protein encoded by the human MDR-1 gene, is a member of the large ATP-binding cassette (ABC) family of membrane proteins [6]. P-gp, when overexpressed in cancer cells, is able to pump anticancer drugs out of the cells [7-9]; therefore, research efforts have been directed to the search of P-gp deactivators in order to ensure an improved prognosis in cancer treatment.

The mammalian thioredoxin reductases (TrxRs or TXNRD1) are a family of selenium-containing pyridine nucleotide-disulfide oxidoreductases [10]. The TrxR system plays a vital role in regulating antioxidant defense and gene transcription [11-13]. TrxR, which is considered to play an important role in carcinogenesis, is overexpressed in numerous types of human tumors, and plays a key role in regulating intracellular redox balance [14]. Over the course of the past few years, an increasing number of studies have attempted to address the role of the thioredoxin (Trx) system in the biology of human malignant tumors, and a large amount of evidence derived

from studies carried out in the laboratory and clinical setting have verified that the TrxR/Trx system is a putative target for antitumor drug development [15-17]. As expected, the expression of TrxR/Trx in various types of tumor has been demonstrated to be higher compared with that in corresponding non-cancerous tissues [18-20]. Previous studies have reported that the expression of Trx/TrxR in tumor cells is increased following treatment with chemotherapeutic drugs, including cisplatin (CDDP), and this has been demonstrated to be associated with drug resistance [21, 22]. Since TrxR is the only enzyme that is known to catalyze the reduction of oxidized Trx, it has been inferred that TrxR may serve as a protector against chemotherapeutic drugs [23]. Therefore, we hypothesized that antagonists of TrxR may contribute towards improving the efficacy of chemotherapeutic drugs, thereby preventing the development of MDR.

CDDP, a potent antitumor agent, has been widely used in numerous types of cancer chemotherapies, including ovarian, bladder, esophageal, testicular and head-and-neck cancer, small lung cancer, and NSCLC [24, 25]. It is the most active chemotherapeutic drug known against NSCLC. However, CDDP resistance often occurs in clinical therapy [26]. This resistance may arise as a consequence of multiple complications, including a reduced drug intracellular concentration, an altered intracellular drug distribution, decreased drug-target interaction, strengthened DNA-damage repair, cell-cycle deregulation, enhanced detoxification responses and an attenuated apoptotic response [27]. The human multidrug-resistant cell line,

A549/CDDP, exhibits a 5.49-fold CDDP resistance against its parental cell line, which is a potent level of CDDP resistance. This cell line may be used in studies *in vitro* for the direct assessment of the MDR phenomenon, such as in the case of the overexpression of P-gp. The inhibition of P-gp may increase the intracellular drug concentration and enhance NSCLC apoptosis.

The extracellular signal-regulated kinase (ERK), signal transducer and activator of transcription 3 (STAT3), AKT and nuclear factor (NF-κB) pathways have been reported to be closely associated with durgs resistances, including cisplatin (CDDP) resistance [28-31]. Essentially, inhibition of ERK, STAT3, AKT and NF-κB can induce cell apoptosis and activate PARP and caspase-3 [32-35]. Importantly, activation of NF-κB can enhance P-gp expression [36], while attenuating NF-κB suppresses P-gp expression [37].

CDDP is the first-line chemotherapy treatment for NSCLC in clinic. By forming the DNA adducts, CDDP inhibits cancer cells viability and the DNA replication. Overexpression of excision repair cross-complementary1 (ERCC1) in tumour cells cleans this cisplatin induced DNA adducts, and brings about CDDP resistance. Therefore, targeting ERCC1 can reverse CDDP resistance in NSCLC cells [38].

Oleanolic acid (OA) is a well-known natural triterpenoid that has numerous pharmacological functions in anti-inflammatory, antivirus, anti-microbial and

anti-parasitic processes, and so forth [27, 39]. The OA derivatives, 2-cyano-3,12-dioxoolean-1,9-dien-28-oic acid (CDDO) and CDDO-Me (its methylated derivative), have been shown to exhibit potent anticancer activities [40-42]. Previous studies have demonstrated that several OA derivatives target MDR by suppressing ABCB1 expression, whereas OA itself inhibits multidrug resistance protein (MRP1 or ABCC1) instead of ABCB1 [43]. In our previous study, we obtained a novel synthesized OA family compound, olean-28,13b-olide 2 (OLO-2), and demonstrated that it exhibits selective cytotoxic activity by inducing the apoptosis of human hepatocellular carcinoma cell lines, but not that of normal human hepatic cells in vitro [44]. The present study aimed to investigate the multiple pharmacological activities of OLO-2 in multidrug-resistant NSCLC cells.

2. Materials and methods

2.1. Reagents and chemicals

OLO-2 (purity, >99%) was first designed and synthesized by the authors of the present study [45]. The molecular structure is illustrated in Fig. 1A. OLO-2 and CDDO-ME were synthesized in our laboratory, dissolved in DMSO at a concentration of 10 mM, and stored at -20°C until further use. The stock solution was diluted to the appropriate concentration in culture medium containing serum immediately prior to addition to the cell cultures.

All antibodies were purchased from Abcam (Cambridge, UK), Cell Signaling Technology, Inc. (Danvers, MA, USA) and ProteinTech Group, Inc. (Chicago, IL,

USA). Cisplatin was purchased from QiLu Pharmaceuticcal (Jinan, China). Rhodamine 123, N-acetyl-L-cysteine-antioxygen (NAC), thiazolyl blue tetrazolium bromide (MTT) and dimethylsulfoxide (DMSO) were purchased from Sigma-Aldrich (Darmstadt, Germany). A Pgp-Glo™ Assay system was purchased from Promega Corp. (Madison, WI, USA). RPMI-1640 medium and fetal bovine serum (FBS) were from Gibco (now a brand of Thermo Fisher Scientific, Inc, Waltham, MA, USA). The reagents RTA 408, S3I 201, U0126, zVAD-fmk, LY 294002, glutathione (GSH), doxorubicin, vincristine and paclitaxel were all purchased from Selleck Corporation (Houston, TX, USA).

2.2. Cell culture

The human lung adenocarcinoma cell lines, A549, SPC-A-1 and LTEP-a-2, the multidrug resistant human lung adenocarcinoma cell line, A549/CDDP, and the human bronchial epithelial cell line, HBE (obtained from the Cell Biology Research Laboratory of Modern Analysis and Testing Center of Central South University, Changsha, China), were cultured in our laboratory. The cells were cultured in RPMI-1640 medium supplemented with 10% FBS, 100 U/ml penicillin, and 100 mg/ml streptomycin at 37˚C under a humidified atmosphere with 5% CO_2. To maintain drug resistance, the A549/CDDP cells were cultured with 4 μg/ml CDDP, and subsequently cultured in CDDP-free RPMI 1640 medium for 2 days prior to the start of the experiments.

2.3. MTT assay.

A total of $1x10^4$ cells in 200 µl of cell culture medium were seeded into each well of a 96-well plate. Following incubation in 5% CO2 at 37˚C for 24 h, the cells were treated with OLO-2, CDDO-Me CDDP and the vehicle, DMSO (0.1%, v/v) alone for 72 h. Subsequently, 20 µl of MTT (5 mg/ml in PBS) was added to each well, and the cells were incubated for a further 4 h, as previously described [46]. The MTT formazan formed by viable cells was dissolved in DMSO (150 µl), and the absorbance at 570 nm was measured using a microplate reader (PerkinElmer VICTOR X3, USA).

2.4. Analysis of cell apoptosis

An Annexin V-Fluorescein Isothiocyanate (FITC) Apoptosis Detection kit (BD Biosciences, Franklin Lakes, NJ, USA) was used for the analysis pf cell apoptosis. A total of $1x10^5$ A549/CDDP cells were seeded into each well of a 6-well plate and treated with the vehicle, DMSO (0.1%, v/v) alone, or with OLO-2 or CDDO-ME for 48 h. The cells were then collected and resuspended in 100 µl 1X binding buffer. Aliquots of 5 µl annexin V and propidium iodide (PI) were subsequently added to the buffer, according to the manufacturer's instructions. Finally, the cells were analyzed by flow cytometry using a BD FACSCanto™ cell analyzer (BD Biosciences), as previously described [47].

2.5. Western blot analysis

The total cellular proteins from the A549/CDDP or A549 cells exposed to OLO-2 , CDDO-ME and the vehicle, DMSO (0.1%, v/v) alone were extracted and quantified

using a bicinchoninic acid (BCA) kit (Thermo Fisher Scientific, Inc., Waltham, MA, USA), according to the manufacturer's instructions. The protein samples (20 μg) extracted from the A549/CDDP or A549 cells were resolved by electrophoresis on 10, 12 or 15% polyacrylamide gels, and electro-transferred onto nitrocellulose membranes. After blocking with 5% non-fat dry milk in PBS containing 0.01% Tween-20 (T-PBS), the membranes were blotted with antibodies against extracellular-signal-regulated kinase (ERK) (16443-1-AP, Proteintech), phosphorylated (p)-ERK (#4370, Cell Signaling Technology), nuclear factor-κB (NF-κB) (10745-1-AP, Proteintech), p-NF-κB (#3033, Cell Signaling Technology), signal transducer and activator of transcription 3 (STAT3) (60199-1-Ig, Proteintech), p-STAT3 (#9134, Cell Signaling Technology), AKT (10176-2-AP, Proteintech), p-AKT (#4060, Cell Signaling Technology), H2A.X (ab11175, Abcam), Ser15-p53 (#9286, Cell Signaling Technology), Ser20-p53 (#9287, Cell Signaling Technology), TrxR （#6925, Cell Signaling Technology）, caspase-3 (#9662, Cell Signaling Technology), c-caspase-3 (#9661, Cell Signaling Technology), PARP (13371-1-AP, Proteintech), c-PARP (SAB4500488, Sigma-Aldrich), alpha-tubulin (T6074, Sigma-Aldrich), β-actin (7D2C10, Proteintech), ERCC1 (66275-1-Ig, Proteintech) and P-gp (#13342, Cell Signaling Technology), respectively. The blots were washed in T-PBS 3 times. Subsequently, they were developed with horseradish peroxidase (HRP)-labeled anti-rabbit immunoglobulin (Ig)G or anti-mouse IgG secondary antibodies for 45 min at room temperature. After washing 3 times in T-PBS, signals were detected using an enhanced chemiluminescence system (EMD Millipore,

Billerica, MA, USA). The images were captured with the Bio-Rad Imaging System, as previously described [48].

2.6. Measurement of P-gp and TrxR mRNA expression

Following treatment with 1.25 μM, 2.5 μM and 5 μM OLO-2, 5 μM CDDO-ME or the vehicle, DMSO (0.1%, v/v) alone for 48 h, the A549/CDDP cells ($1x10^5$) were digested in TRIzol® reagent (Invitrogen/Thermo Fisher Scientific, Inc., Waltham, MA, USA), and total RNA was extracted according to the manufacturer's instructions and as previously described [49].

A sample (1 μg) of RNA was then reverse transcribed by oligo-dT primer using a RevertAid First Strand cDNA Synthesis kit (Thermo Fisher Scientific, Inc., Waltham, MA, USA) following the manufacturer's instructions and as previously described [50]. Aliquots of 1 μl cDNA were used as the template for polymerase chain reaction (PCR) using the following primers: ABCB1 forward, 5'-CCTTCAGGGTTTCACATTTGGC-3'; ABCB1 reverse, 5'-ATCATTGGCGAGCCTGGTAG-3'; TXNRD1 forward, 5'-GCAGACGAAAGGCAAGAACG-3'; TXNRD1 reverse, 5'-TCTTTACCTCAGTACAGCGTGTG-3'; GAPDH forward, 5'-GATGACATCAAGAAGGTGGTGA-3'; and GAPDH reverse, 5'-GTCTACATGGCAACTGTGAGGA-3'. The PCR conditions used were 34 cycles of denaturation (94° C, 1 min), annealing (60°C, 30 sec) and polymerization (72°C, 1 min). The standard curves were generated, and data analyses were performed using

Bio-Rad iQ5 software (Bio-Rad). The relative ABCB1 and TXNRD1 mRNA levels treated with OLO-2 were expressed as fold changes of the control (in the presence of 0.1% DMSO).

2.7. Measurement of TrxR activity by cell-free and cellular assays.

TrxR (0.5 μM) and nicotinamide-adenine dinucleotide phosphate (NADPH; 100 μM) were mixed together in TE buffer in 96-well plates, and incubated at room temperature for 5 min. Subsequently, a series concentrations (0.3125, 0.625, 1.25, 2.5, 5 and 10 μM) of OLO-2, CDDO-ME, or DMSO (0.1%, v/v) alone were added, and the mixtures were incubated in quadruplicate at room temperature for 2 h in a final mixture volume of 80 μl. To measure the TrxR activity, 60 μl of the mixture was withdrawn by plus guns and added to a cuvette containing 25 μl 4 mM NADPH and 2 mM 5,5'-dithiobis(2-nitrobenzoic acid) (DTNB). The absorbance at 412 nm was measured with a spectrophotometer (PERSEE, T6, Beijing, China) at 1 min after initially mixing with a blank reference.

The Thioredoxin Reductase Assay kit (Cayman Chemical Co., Ann Arbor, MI, USA) was used to measure the inhibition of TrxR activity by OLO-2, CDDO-ME, or DMSO (0.1%, v/v) alone in the A549 and A549/CDDP cells. In brief, the cells were cultured in the presence of 1.25, 2.5, 5, 10, 25 and 50 μM OLO-2 or CDDO-ME, or DMSO (0.1%, v/v) alone for 24 h. Subsequently, the cells were lysed in RIPA buffer (Beyotime Institute of Biotechnology, China) in the presence of protease inhibitor (Thermo Fisher Scientific, Inc., Waltham, MA, USA). After quantifying the protein

concentrations, 50 μg cell protein per sample was reacted in quadruplicate with NADPH (40 mg/ml) and DTNB (10 mM) in TE buffer in 96-well plates at 37℃ for 1 h. The absorbance was then measured using a microplate spectrophotometer (Berthold, LB941, Germany) at 412 nm. The inhibition rate of TrxR was calculated based on the ratio of activity difference between the control group (DMSO alone) and the experimental group.

2.8. P-gp ATPase assay

P-gp ATPase assay was performed according to the instructions for use provided by Pgp-Glo™ Assay systems (Promega Corp., Madison, WI, USA). Briefly, the individual P-gp membrane samples (250 μg/ml) were treated in quadruplicate at 37°C for 60 min with 40 μM OLO-2, 200 μM verapamil (substrate control), 200 μM Na_3VO_4 (P-gp inhibitor) or the vehicle in the presence of 5 mM MgATP. After the completion of the above-mentioned reaction, 50 μl of ATP detection reagent were added to each sample, respectively, followed by an incubation at room temperature for 20 min. The relative light units (RLUs) in individual samples were measured using a luminescent detector (Beckman Coulter, Inc., Brea, CA, USA). RLUs representing the quantity of ATP consumed by P-gp-ATPase were detected using a luminescent detector, and RLUs were obtained from the untreated samples ($RLU_{untreated}$), verapamil-treated samples (RLU_{VRP}), Na_3VO_4-treated samples (RLU_{Na3VO4}) and OLO-2-treated samples (RLU_{OLO-2}) (Table III), using the following formulae: RLU_{Na3VO4} - $RLU_{untreated}$ = ΔRLU_{basal} (ΔRLU_{basal} reflects basal P-gp-ATPase activity);

RLU_{Na3VO4} - RLU_{OLO-2} = ΔRLU_{OLO-2} (ΔRLU_{OLO-2} reflects P-gp-ATPase activity in the presence of OLO-2). $\Delta RLU_{OLO-2} > \Delta RLU_{basal}$ indicated that OLO-2 was a stimulator of Pgp ATPase activity; $\Delta RLU_{OLO-2} = \Delta RLU_{basal}$ indicated OLO-2 has no effect on Pgp ATPase activity; and $\Delta RLU_{OLO-2} < \Delta RLU_{basal}$ indicated that OLO-2 is an inhibitor of Pgp ATPase activity. Na_3VO_4 is an inhibitor of P-gp-ATPase, and is often used as a negative control.

2.9. Fluorescence microscopy observation of intracellular Rhodamine 123

A total of $1x10^5$ A549/CDDP cells or A549 cells were seeded in each well of 6-well plates 24 h prior to the experiment. The cells were treated with various concentrations of OLO-2 (0.625, 1.25, 2.5 and 5 μM), verapamil (5 μM) or the vehicle DMSO (0.1%, v/v) alone for 2 h at 37℃. To assess the accumulation of Rhodamine 123, 5 μM Rhodamine 123 was added to each cell culture, followed by incubation for 1 h in the dark at 37℃. After washing the cells 3 times with cold PBS, images were captured using a fluorescence microscope (Nikon Corp., Tokyo, Japan).

2.10. Effect of OLO-2 on the P-gp-mediated efflux of Rhodamine 123

Cell suspensions with $1x10^5$ cells/ml were treated with various concentrations of OLO-2 (0, 0.625, 1.25, 2.5 and 5 μM), verapamil (5 μM) or the vehicle, DMSO (0.1%, v/v) alone for 2 h at 37°C. Subsequently, the cells were collected by centrifugation at 300 x g and washed twice with cold PBS. In order to assess the extent of the accumulation of Rhodamine 123, 5 μM Rhodamine 123 were added, and the cells

were incubated for 1 h in the dark at 37℃. Finally, the cells were washed 3 times with cold PBS and resuspended in PBS buffer prior to analysis by flow cytometry using a BD FACSCanto™ cell analyzer (BD Biosciences) equipped with an excitation wavelength of 488 nm and an emission wavelength of 590 nm. The data were analyzed using Flowjo version 10 software.

2.11. OLO-2 enhances CDDP-induced A549/CDDP cell apoptosis by triggering caspase-3

To confirm the effect of caspase-3 in OLO-2 and CDDP mediated A549/CDDP cells apoptosis, 40 μM of the pan-caspase inhibitor, zVAD-fmk, was added into the medium before the treatment of 20 μM CDDP and 1μM OLO-2. After the combined treatment for 48 h, flow cytometry and western blot were used to examine the effects.

2.12. Measurement of ROS generation

The A549/CDDP cells were incubated with the vehicle [DMSO (0.1%, v/v)] alone, 1 μM OLO-2, 20 μM CDDP, or a combination of 1 μM OLO-2 and 20 μM CDDP for 2 h. Subsequently, the cells were stained with dihydroethidium (DHE; Beyotime Institute of Biotechnology, Haimen, China), which could mark the cells as the probe of O_2^-, a kind of primary ROS, as previously described [51, 52]. The levels of intracellular ROS were detected by measuring the fluorescence signals using a fluorescence microplate reader (absorbance, 610 nm) (PerkinElmer VICTOR X3, USA).

To determine the role of intracellular ROS in the apoptotic cell death induced by combined treatment with OLO-2 and CDDP, both *N*-acetyl-L-cysteine-antioxygen (NAC) and glutathione (GSH) ROS scavengers were used. A549/CDDP cells were pre-treated with 10 mM NAC or GSH for 2 h before the combined treatment with 1 μM OLO-2 and 20 μM CDDP. After 72 h combined treatments, MTT assays were used for detecting the combinations against A549/CDDP viability.

2.13. Measurement of the combination with Inhibtors of the PI3K/AKT, MEK/ERK, NFκB and STAT3 pathways

A549/CDDP cells were respectively pre-treated with 10 μM LY294002 (an upstream inhibitor of AKT), U0126 (an ERK inhibitor), 1 μM RTA 408 (a specific NF-κB inhibitor), or 60 μM S3I 201 (a STAT3 inhibitor) for 2 h prior to the combined treatment with CDDP and OLO-2 or the vehicle, DMSO (0.1%, v/v). Cell viability was detected by MTT assay and western blot. After 48 h, the cells were detected by western blot, and Cell viability was examined by MTT assay after 72 h.

2.14. Measurement of CDDP with Inhibitors of PI3K/AKT, MEK/ERK, NFκB and STAT3 pathways

A549/CDDP cells were pre-treated with 10, 20, 30 μM LY294002 and U0126, respectively, or 1, 2, 3 μM RTA 408, or 60, 120, 180 μM S3I 201 for 2 h prior to the combined treatment with 20 μM CDDP. After 72 h, Cell viability was detected by MTT assay.

2.15. Cell transfection

In order to silence TXNRD1, the A549/CDDP cells were transfected with non-targeting siRNA (RioboBio, China) or siRNA-TXNRD1, of which sequence is GCAAGACTCTCGAAATTAT, using Lipofectamine™ 3000 reagent (Thermo Fisher Scientific, Inc., Waltham, MA, USA). Briefly, the cancer cells ($2x10^5$) were plated into a 60 mm Petri dish, cultured for 24 h, and treated with 4 ml Opti-MEM™ medium containing 10 μl Lipofectamine™ 3000 reagent and 100 nM siRNA for 48 h (51). TrxR expression was subsequently analyzed by Realtime PCR and western blot analysis.

For the overexpression of TXNRD1, the A549/CDDP cells were transfected with 10 μg empty or TXNRD1 expression plasmid (pcDNA-3.1-TXNRD1) using Lipofectamine™ 3000 reagent. Following transfection for 48 h, the cells were examined for TrxR expression by western blot analysis.

2.16. Statistical analysis

Each experiment was repeated at least 3 times, and the data are presented as the means ± standard deviation (SD). Differences were analyzed by a Student's t-test using SPSS version 18.0 statistical software (SPSS, Inc., Chicago, IL, USA). For larger datasets involving >2 groups, one-way analysis of variance (ANOVA) with Bonferroni's multiple comparison tests was used. A value of $P \leq 0.05$ was considered to indicate a statistically significant difference.

3. Results

3.1. OLO-2 inhibits the proliferation of human lung adenocarcinoma cells in vitro

Four human lung adenocarcinoma cell lines were examined by MTT assay. OLO-2 significantly inhibited the proliferation of the human lung adenocarcinoma cells, and the inhibition ratio increased in a dose-dependent manner (Fig. 1B, C, D and E). At the majority of concentrations, the inhibition ratios of OLO-2 in four species of lung adenocarcinoma cells were significantly higher than the human normal bronchial epithelial cell line, HBE (Fig. 1B, C, D and E), suggesting that OLO-2 is a selective anticancer compound against human lung adenocarcinoma cells ($P<0.01$). The IC_{50} (i.e., the concentration at which cell viability is inhibited by 50%) values of OLO-2 following 72 h of treatment of the human lung adenocarcinoma cells are presented in Table I. The IC_{50} values of OLO-2 were comparable with the IC_{50} values of the positive controls, CDDP and CDDO-Me (a C-28 methyl ester of CDDO). In addition, OLO-2 exerted a similar inhibitory effect on the A549/CDDP (2.39±0.56 μM) and A549 (1.96±0.41μM) cells, thereby exhibiting an advantage over CDDP and CDDO-ME. These data indicate that OLO-2 may have potential for use as a treatment agent against human MDR lung adenocarcinoma cells.

3.2. OLO-2 inhibits TrxR mRNA and protein expression

Various types of tumor cells are able to overexpress TrxR/Trx proteins in order to

maintain tumor survival [14], and this overexpression has been shown to be associated with clinical outcomes, including irradiation [53, 54] and drug resistance [21, 22]. Inhibition of TrxR induces ROS rising[54, 55], which can lead to DNA damage [56] and cell apoptosis. Therefore, western blot and RT-PCR analyses were used to determine whether the inhibition of multidrug resistant human lung adenocarcinoma cells induced by OLO-2 was caused by effect on TrxR. First, TrxR protein expression was detected among the A549, A549/CDDP and HBE cell lines. As shown in Fig. 2A and B, both cancer cell lines exhibited a significantly higher TrxR expression compared with the normal cell line, HBE, and the A549/CDDP cells expressed ~4-fold the levels of TrxR protein compared with the A549 cells. Subsequently, treatment of the A549/CDDP cells with OLO-2 markedly decreased TrxR protein and mRNA expression (Fig. 2C-E), although CDDO-ME did not lead to a decrease in TrxR expression at either the protein or mRNA levels. As the concentration of OLO-2 increased, the levels of TrxR protein and mRNA expression decreased. And we find that Trx protein was affected by OLO-2 too (Fig. 2C). As the concentration of OLO-2 increased, the inhibition rates of TrxR protein and mRNA expression also increased. These results suggested that TrxR is indeed a target of OLO-2.

3.3. OLO-2 inhibits TrxR in both cell-free and cellular assays

The results described above demonstrated that OLO-2 could inhibit TrxR expression. For the further study, we wished to determine whether OLO-2 inhibits

TrxR activity. First, the inhibitory effects of OLO-2 and CDDO-ME on the purified TrxR enzyme were examined with a DTNB assay, which could furnish a direct measurement of TrxR activity[23, 57]. As shown in Table II, OLO-2 exhibited more marked TrxR inhibitory activity (IC_{50}, 0.95 μM) compared with CDDO-ME (IC_{50}, 2.71 μM). Secondly, the TrxR inhibitory activity of OLO-2 and CDDO-ME in the A549 and A549/CDDP cells was detected. In brief, the cells were treated with various concentrations of OLO-2 or CDDO-ME for 24 h, and the activity of TrxR was measured using a Thioredoxin Reductase Assay kit [58]. As shown in Table II, OLO-2 displayed significantly more potent TrxR inhibitory activity (IC_{50}, 4.49 and 3.14 μM, A549 and A549/CDDP cells, respectively) compared with CDDO-ME (IC_{50}, 13.12 and 13.39 μM, A549 and A549/CDDP cells, respectively) ($P<0.05$). These results indicated that OLO-2 may function as a TrxR inhibitor to suppress cell survival.

3.4. OLO-2 inhibits P-gp expression and activity in A549/CDDP cells.

The results of fluorescence microscopy and flow cytometric analysis demonstrated that, with an increase in the OLO-2 concentration, the inhibition of P-gp became more pronounced, and even at the concentration of 2.5 μM, OLO-2 exerted more marked effects than did 5 μM verapamil, using the P-gp substrate, Rhodamine 123, as an indicator (Fig. 3C and G). A previous study demonstrated that cancer cells expressing P-gp may exhibit drug resistance [59]. The inhibition of cellular P-gp expression may therefore enhance the sensitivity of cancer cells to chemotherapeutic drugs [60, 61]. In

this study, to further reveal whether the multi-targeted agent, OLO-2, inhibits P-gp expression and activity in A549/CDDP cells, western blot analysis was used to examine P-gp expression in the A549/CDDP and A549 cell lines following treatment with OLO-2. As shown in Fig. 3A and B, the A549/CDDP cells expressed high levels of P-gp; however, the A549 cells only exhibited weak levels of P-gp protein expression. Following treatment with OLO-2, the mRNA and protein levels of P-gp were clearly inhibited in the A549/CDDP cells, as determined by RT-PCR and western blot analysis (Fig. 3D, E and F).

3.5. Evaluating the effects of OLO-2 on P-gp-ATPase activity in vitro.

The Pgp-Glo™ Assay system was used to directly investigate the effects of OLO-2 on P-gp-ATPase. P-gp pumps drugs out of the cells by consuming ATP, and the quantity of the ATP consumption may reflect whether the compound is a stimulator or an inhibitor of P-gp-ATPase activity. Verapamil is a substrate of P-gp, which has been identified to be a stimulator of P-gp-ATPase and can be used as a positive control. According to the calculated results, OLO-2 was demonstrated to be an inhibitor of P-gp ATPase activity (Table III).

3.6. OLO-2 enhances CDDP-induced ROS accumulation

Inhibition of TrxR can induce ROS accumulation[54, 55], and CDDP has been reported to generate ROS to induce cell death as a part of its anticancer defense mechanism [62]. We therefore wished to determine whether OLO-2 can

synergistically enhance the ROS levels induced by CDDP. As was anticipated, treatment with OLO-2 alone elicited detectable ROS overproduction in a time-dependent manner, as measured using the fluorescein-labeled probe, DHE (Fig. 4A). Furthermore, co-treatment with OLO-2 and CDDP markedly elevated the CDDP-induced ROS levels in a time-dependent manner, and the ROS levels markedly increased during the period between 0-20 min, suggesting an important participatory role of ROS in the early stages of triggering cell apoptosis (Fig. 4A). The excessive ROS levels may further induce intracellular DNA damage and activate downstream signaling pathways.

In addition, both *N*-acetyl-L-cysteine (NAC)-antioxygen and glutathione (GSH) ROS scavengers were used to determine the role of intracellular ROS in the apoptotic cell death induced by combined treatment with OLO-2 and CDDP. As was expected, the addition of GSH and NAC attenuated the suppressive effects on A549/CDDP cell proliferation induced by combined treatment with OLO-2 and CDDP (Fig. 4B). The cells treated with a combination of 20 μM CDDP and 1 μM OLO-2 exhibited a decrease in viability to 35.7%. However, treatment of the cells with 10 mM NAC or 10 mM GSH for 2 h prior to combined treatment with OLO-2 and CDDP significantly increased cell viability to 65.2 and 70.2%, respectively. NAC and GSH reversed the suppressive effects on the apoptosis of the A549/CDDP cells induced by combined treatment with OLO-2 and CDDP, implying that ROS production is essential for the induction of cell apoptosis resulting from combined treatment with OLO-2 and CDDP.

3.7. DNA damage is triggered by OLO-2 alone and combination treatment with OLO-2 and CDDP.

Accumulation of the ROS can lead to DNA damage [56]. To determine whether the combination of OLO-2 and CDDP induces DNA damage, DHE and 3 DNA damage markers, H2A.X, p-p53 (Ser-20) and phosphorylation of histone (Ser-15), were examined to investigate this synergistic effect. Treatment with OLO-2 or CDDP alone activated H2A.X and p-p53 in the A549/CDDP cells (Fig. 4C and D). However, the combination of OLO-2 and CDDP markedly enhanced CDDP-induced DNA damage, as indicated by the enhanced H2A.X activation and p53 phosphorylation (Fig. 4C and D). Finally, the effects of the combined treatment were attenuated by pre-treatment of the cells with GSH for 2 h (Fig. 4C and D).

3.8. OLO-2 alone inhibits the PI3K/AKT and MEK/ERK pathways, and augments the CDDP-induced inhibition of the PI3K/AKT and MEK/ERK pathways

DNA damage can lead to the inhibition of the PI3K/AKT and MEK/ERK pathways [63, 64]. Phosphoinositide 3-kinase (PI3K)/AKT and mitogen-activated protein kinases (MAPKs, including ERK) both serve as upstream kinases in their respective signaling pathways, and play vital roles in regulating cell survival, proliferation and cell growth [65, 66]. In this study, important signaling molecules in the PI3K/AKT and MAPK pathways, including AKT, p-AKT (Ser-473), ERK and p-ERK (Thr-202/Tyr-204), were investigated to evaluate the role of OLO-2-associated

mechanisms in inhibiting cell survival. The results obtained from western blot analysis demonstrated that treatment with OLO-2 alone led to obvious downregulation of AKT, p-AKT and p-ERK (Fig. 5A, D, E and I). Combined treatment with OLO-2 and CDDP markedly inhibited AKT and ERK activation to an even greater extent. Subsequently, LY 294002 and U0126, specific inhibitors of AKT and ERK respectively, were used to further verify the roles of AKT and ERK in inducing the death of A549/CDDP cells by combined treatment of OLO-2 and CDDP. The results revealed that pre-treatment with the two inhibitors for 2 h significantly augmented the inhibitory effects on A549/CDDP cell viability induced by combined treatment (Fig. 6A). Furthermore, the dephosphorylation of ERK and AKT induced by combined treatment was enhanced by pre-treatment with the inhibitors, LY294002 and U0126, for 2 h (Fig. 6C and D). These results demonstrated that combined treatment with OLO-2 and CDDP inhibited A549/CDDP cell growth in an ERK- and AKT-dependent manner. OLO-2, as well as the investigated inhibitors of ERK and AKT signaling, acted synergistically with CDDP to reduce A549/CDDP cell viability.

3.9. OLO-2 alone inhibits STAT3 pathways, and enhances the CDDP-induced inhibitory effects on the NF-κB and STAT3 pathways

DNA damage can also suppress NF-κB and STAT3 pathways [67, 68]. NF-κB and STAT3 are closely associated with tumor cell survival, proliferation and invasion, and are targets for drug development and cancer therapy [23, 69-71]. In this study, to determine whether OLO-2 inhibits activation of the NF-κB and STAT3 pathways, the

expression of NF-κB, p-NF-κB (Ser-536), STAT3 and p-Stat3 (Ser-727) was investigated. The results indicated that OLO-2 alone suppressed the protein levels of p-STAT3 (Ser-727) (Fig. 5A and G) and the inhibition of NF-κB was not obviously when treated with 1μM OLO-2 alone (Fig. 5A). However, NF-κB pathway could be blocked via DNA damage caused by the increase in ROS upon OLO-2 treatment. Additionally, combined treatment with OLO-2 and CDDP markedly inhibited NF-κB and STAT3 activation (Fig 5A, B, C, F and G). To further confirm the roles of NF-κB and STAT3, cell viability was detected by MTT assay using the specific NF-κB and STAT3 inhibitors, RTA 408 and S3I 201, respectively. The results revealed that pre-treatment with the two inhibitors for 2 h markedly enhanced the inhibitory effects on A549/CDDP cell growth induced by combined treatment with OLO-2 and CDDP (Fig. 5B). The dephosphorylation of ERK and AKT induced by combined treatment with OLO-2 and CDDP was markedly augmented by pre-treatment with the inhibitors, RTA 408 and S3I 201, for 2 h (Fig. 5E and F). Taken together, these data demonstrated that, in addition to the PI3K/AKT and MEK/ERK pathways, the NF-κB and STAT3 signaling pathways also play important roles in the inhibition of A549/CDDP cell growth induced by combined treatment with OLO-2 and CDDP.

3.10. Inhibitions of PI3K/AKT, MEK/ERK, NFκB and STAT3 pathways can reverse CDDP resistance

It has been reported that *PI3K/AKT, MEK/ERK, NFκB and STAT3 pathways* are closely associated with durgs resistances, including cisplatin (CDDP) resistance

[28-31]. We wish to determine whether attenuating four pathways could reverse CDDP resistance. We used the inhibitors of the four pathways to suppress the pathways, respectively, and MTT assay was used to examine A549/CDDP cells viability with 20 μM CDDP treatment.

The results showed that 30 μM LY 294002 (an upstream inhibitor of AKT) or U0126 (an ERK inhibitor) could obviously sensitize A549/CDDP cells to the CDDP treatment (Fig. 7A and B), and 180 μM S3I 201 (a STAT3 inhibitor) or 3 μM RTA 408 (a specific NF-κB inhibitor) could also achieve this effect (Fig. 7C and D). Because the combination of OLO-2 and CDDP significantly suppressed the four pathways, the combined treatment should be able to reverse CDDP resistance through this mechanism.

3.11. OLO-2 induces the apoptosis of A549/CDDP cells

To determine whether the inhibitory effects of OLO-2 on the proliferation of human multidrug resistant lung cancer cells were accompanied by enhanced apoptosis, Annexin V-FITC and PI staining was applied to evaluate the percentages of apoptotic cells by flow cytometric analysis. The results revealed that the apoptotic rate induced by OLO-2 in the A549/CDDP cells was significantly higher compared with that induced by CDDO-ME or CDDP ($P < 0.01$; Fig. 8A and B).

In addition, the results of western blot analysis revealed that treatment with 1 μM OLO-2 for 48 h markedly decreased the levels of pro-caspase-3 and PARP, but evidently increased cleaved-caspase-3 and cleaved-PARP expression in the

A549/CDDP cells (Fig. 8E and F), also indicating that OLO-2 induced the apoptosis of the A549/CDDP cells.

3.12. OLO-2 enhances CDDP-induced A549/CDDP cell apoptosis by triggering caspase-3 activation

The apoptotic rate was 12.37% in the A549/CDDP cells treated with 20 μM CDDP (Fig. 7E). It was noteworthy that treatment with a combination of 1 μM OLO-2 and 20 μM CDDP for 48 h markedly enhanced cell apoptosis to 27.54%, and cell necrosis to 38.9% (Fig. 8C). However, when the cells were pre-treated with 40 μM of the pan-caspase inhibitor, zVAD-fmk, for 2 h, the apoptosis induced by 1 μM OLO-2 and 20 μM CDDP was markedly decreased ($P<0.05$; Fig. 8C and D).

To further investigate the mechanisms responsible for the enhancement of the CDDP-induced apoptosis of A549/CDDP cells by OLO-2, western blot analyses were performed. The cells were treated with 20 μM CDDP or 1 μM OLO-2 individually or in combination for 48 h. CDDP induced the activation of caspase-3 and the cleavage of PARP, and the effects of OLO-2 were as described above (Fig. 8E and F). Combined treatment with OLO-2 and CDDP significantly decreased the expression of pro-caspase-3 and PARP, and markedly increased cleaved caspase-3 and cleaved PARP expression (Fig. 8E and F). To verify the role of caspase-3 in the enhancement of CDDP-induced A549/CDDP cell apoptosis by OLO-2, the cells were treated with 40 μM of the pan-caspase inhibitor, zVAD-fmk, for 2 h prior to the various combination treatments. The results demonstrated that the cleavage of caspase-3 and

PARP induced by the combined treatments was impeded by zVAD-fmk (Fig. 8E and F). Thus, we hypothesized that caspase-3 activation may play a critical role in the apoptosis of A549/CDDP cells which was induced by CDDP and enhanced by OLO-2.

3.13. Role of TrxR in OLO-2 treatment.

To further investigate the role of TrxR in the OLO-2-induced inhibition of cell proliferation and survival, siRNA and transfection technologies were used to knock down or overexpress TrxR in the A549 and A549/CDDP cells upon treatment with various concentrations of OLO-2 for 48 h. After identifying alterations in the TrxR protein levels by western blot analysis, the cell death was measured by MTT assay. As shown in Fig. 9A, transfection with siRNA-TrxR markedly enhanced the sensitivity of the two cell lines to OLO-2 at concentrations of 0.25-1.25 μM. On the other hand, the overexpression of TrxR markedly reduced the sensitivity to OLO-2 at concentrations of 0.625-5 μM (Fig. 9B). Transfection with the empty plasmid and the non-targeting siRNA had no effect on the response of cells to OLO-2 (Fig. 10).

Taken together, these results demonstrate that TrxR plays a role in the effects of OLO-2 treatment on human lung adenocarcinoma cells. OLO-2 induces ROS which in turn renders cells dependent on Trx protection. Hence when Trx protection goes down, cell death increases.

3.14. TrxR plays an important role in the resistance of A549/CDDP cells to CDDP.

It is well known that TrxR is usually overexpressed in various types of cancer cells [18, 72], and is associated with the drug resistance of tumors [22]. Thus, in this study. to confirm and compare the resistance of A549/CDDP cells to CDDP by overexpressing or suppressing TrxR, Annexin V and PI flow cytometric analysis was used. Transient transfection with pcDNA-3.1-TXNRD1 markedly increased the viability of the A549/CDDP cells in the presence of 50 μM CDDP (Fig. 9C and D). When CDDP dose increased from 20 to 50 μM, CDDP-induced ROS raised and the CDDP-induced ROS would induce the more cancer cells apoptosis[62]. The raised TrxR expression could reduce ROS harmful effect and decrease the apoptosis which was induced by ROS. By contrast, transfection with siRNA-TXNRD1 markedly increased the sensitivity of the A549/CDDP cells to CDDP at the concentration of 20 μM (Fig. 9C and D).These results indicated that TrxR indeed plays an important role in the resistance of A549/CDDP cells to CDDP, and that the inhibition of TrxR can sensitize the lung cancer cells to CDDP.

CDDP

3.15. OLO-2 inhibits ERCC1 expression in A549/CDDP cells

Overexpressing ERCC1 can cause chemotherapy durg resistances, including CDDP resistance. Chemotherapy durgs induce DNA damage, and ERCC1 can repair this damage [73]. Co-treatment with OLO-2 enhanced CDDP induced DNA damage. We used western blot assay to determine whether the enhancement of DNA damage induced by OLO-2 was caused via ERCC1. As shown in Fig. 11A and B, treatment of

the A549/CDDP cells with OLO-2 obviously decreased TrxR protein expression (Fig. 11 A and B). As the concentration increased, the levels of ERCC1 protein expression decreased. These results indicated that ERCC1 is a target of OLO-2.

In summary, OLO-2 reversed the CDDP resistance and multidrug resistance through the inhibition of thioredoxin and multiple signaling pathways (Fig. 12).

3.16. A549/CDDP cells resist doxorubicin, vincristine and paclitaxel

As a multi-drug resistant cell line, A549/CDDP cells not only resist CDDP but also resist other potent chemotherapeutic drugs. To test A549/CDDP cells' MDR, MTT assay was used to determine the IC_{50} values of doxorubicin, vincristine and paclitaxel, which are first-line chemotherapy drugs. The MTT assay showed that the IC_{50} values of doxorubicin, vincristine and paclitaxel in A549/CDDP cells, respectively, were approximately 50, 15 and 39 fold of the IC_{50} values of them in the parental A549 cells ($P<0.001$) (Table. 4). These results indicated that the A549/CDDP cells in this research are indeed multi-drug resistant cells.

3.17. OLO-2 augments the CDDP-induced inhibition of the PI3K/AKT, MEK/ERK, NF-κB and STAT3 pathways in A549 cells

To test the synergistic effects in the parental A549 cells, MTT and western blot assays were used to determine whether OLO-2 augmeted the cell death and inhibition of the PI3K/AKT, MEK/ERK, NF-κB and STAT3 pathways induced by CDDP. The MTT assay exhibited that the combination of 4 μM CDDP and 0.7 μM OLO-2

exhibited a decrease in viability to 51.29%, which was the most potent effect among all groups (Fig. 11C). The western blot assay showed that combined treatment with OLO-2 and CDDP markedly inhibited p-AKT (Ser 473), p-ERK (Thr 202/Tyr 204), p-NF-κB (Ser-536) and p-Stat3 (Ser-727) expression levels to a significantly greater extent in A549 cells compared to CDDP treatment group (Fig. 11D-H). These results demonstrated that OLO-2 synergizes CDDP-induced growth inhibition of A549 cells and augments the CDDP-induced inhibition of the PI3K/AKT, MEK/ERK, NF-κB and STAT3 pathways.

4. Discussion

CDDP, which is one of the front-line chemotherapeutic drugs used in the treatment of human lung cancer, is often negated by MDR in clinical therapy [74, 75]. OLO-2 targets both TrxR expression and TrxR activity, and this can contribute towards alleviating this critical problem. In this study, when various concentrations of OLO-2 (0.25, 0.5 and 1 μM) were administered to the A549/CDDP cells together with 20 μM CDDP, the apoptotic rates of the cells were found to markedly increase. Combined treatment with CDDP and 1 μM OLO-2 was able to significantly enhance caspase-3 and PARP activation. The inhibitory effects of OLO-2 mediated by TrxR/Trx may prevent Trx from binding to apoptosis signal-regulating kinase 1 (ASK-1), a kinase that plays a vital role in apoptosis and may be inactivated by binding with Trx [76]. If Trx is unable to bind ASK-1, ASK-1 will activate various signaling cascades, ultimately leading to the induction of apoptosis.

P-gp, which has two transmembrane regions and two ATP-binding cassettes, is a famous and the first protein confirmed as a mediator of tumor drug resistance and plays a vital role in MDR progresses in cancer[77]. In this study, OLO-2 was found to inhibit P-gp expression and activity. OLO-2 not only suppresses CDDP resistance but also can reverse the MDR caused by P-gp. We will focus on OLO-2's effect on doxorubicin, a P-gp substrate, and its derivatives in tumor cells in the further research.

The MEK/ERK and PI3K/AKT signaling pathways play essential roles in cell growth, proliferation and survival [78], and activate anti-apoptotic pathways and induce drug resistance in tumor cells [78-80]. Several novel treatment strategies have been developed to inhibit these signaling pathways [81-83]. In the present study, the MEK/ERK and PI3K/AKT pathways were investigated as targets of OLO-2, and OLO-2 was found to synergistically augment the CDDP-mediated apoptosis of human multidrug-resistant lung adenocarcinoma cells by inhibiting ERK and AKT. The results suggested that combined treatment with OLO-2 and CDDP induced the apoptosis of the A549/CDDP cells via AKT- and ERK-dependent mechanisms. In addition, using U0126 (an ERK inhibitor) and LY294002 (an upstream inhibitor of AKT) respectively, inhibitors of the pathways, could sensitize A549/CDDP cells to CDDP, which confirmed that the inhibition of MEK/ERK and PI3K/AKT signaling pathways could weaken the CDDP resistance in the A549/CDDP cells.

NF-κB and STAT3 are closely associated with tumor cell survival, proliferation, invasion and drug resistance [84, 85], and are common targets for drug development and cancer therapy. In the present study, OLO-2 was found to synergistically augment CDDP-mediated death and the apoptosis of human multidrug-resistant lung adenocarcinoma cells by inhibiting the NF-κB and STAT3 signaling pathways. The data demonstrated that the NF-κB and STAT3 pathways also play a key role in the apoptosis of A549/CDDP cells induced by combined treatment with OLO-2 and CDDP. The further study showed that using RTA-408 (a specific NF-κB inhibitor) and S3I-201 (a STAT3 inhibitor) could sensitize A549/CDDP cells to CDDP, which confirmed that the inhibition of NF-κB and STAT3 signaling pathways could diminish the CDDP resistance in the A549/CDDP cells.

Recent studies have demonstrated that the majority of tumor cells, including cancer stem cells, exhibit elevated ROS levels, which render them more vulnerable to increases in oxidative stress levels compared with normal cells, including various types of stem cell [86, 87]. This characteristic may be utilized to selectively induce the apoptosis and death of these cells. CDDP leads to an increase in cellular ROS levels, which provides one of its antitumor mechanisms [88]. In our previous study, OLO-2 was found to be able to induce ROS generation in tumor cells [44]. As was expected, in the present study, the combined use of OLO-2 and CDDP led to a significantly more potent generation of ROS compared with OLO-2 or CDDP treatment alone. Furthermore, the inhibitory effect of this combined treatment was

attenuated by GSH and NAC, which act as ROS scavengers.

Owing to the DNA-damaging effects elicited by ROS, H2A.X, p53-Ser15 and p53-Ser20, three DNA-damage markers that are associated with CDDP treatment [89, 90], were recruited in the present study to assess this effect. The results demonstrated that treatment with OLO-2 and CDDP alone only marginally gave rise to DNA damage in the A549/CDDP cells, as evidenced by the weak upregulation of H2A.X, p53-Ser15 and p53-Ser20. The combination of OLO-2 and CDDP led to a clear enhancement of DNA damage, and the phosphorylation of the DNA-damage markers was attenuated by GSH. Therefore, these results suggest that upregulation of ROS may cause DNA damage, and may further lead to apoptosis.

TrxR and Trx levels are overexpressed in numerous types of tumor cells, particularly those that are treated with chemotherapeutic drugs, such as CDDP, mitomycin C, doxorubicin, docetaxel and etoposide [21, 91-93]. In the present study, the A549/CDDP cells exhibited a marked increase in TrxR expression levels compared with A549 cells. In addition, this study, to the best of our knowledge, demonstrated for the first time, that the overexpression or knockdown of TrxR in A549/CDDP cells may respectively enhance or attenuate the resistance of the cells to CDDP. Therefore, these results indicate that TrxR may function as a protector against chemotherapeutic drugs. TrxR plays vital roles in tumor cells as a redox regulator of intracellular signal transduction and as a free radical scavenger [10, 94, 95]. OLO-2

may inhibit the mRNA and protein expression of TrxR, as well as its activity, which leads to the suppression of Trx, the upregulation of ROS and the apoptosis of human lung adenocarcinoma cells. In this study, it was of interest to ascertain whether OLO-2 exhibits selective toxicity in human lung adenocarcinoma cells compared with human normal cells. We surmised that human lung adenocarcinoma cells require a higher protein expression level of TrxR/Trx than do human normal cells in order to maintain their redox balance for their higher levels of ROS compared with normal cells, and that tumor cells are more vulnerable to TrxR/Trx inhibition than are normal cells. Cancer cells require higher levels of the TrxR/Trx system to dispose of the cellular stress elicited by elevated ROS levels, and to maintain rapid DNA assembly [23, 96].

CDDP can enter into cell nucleus, bind cellular DNA, lead to DNA-platinum adducts and produce inter-strand cross-links, thus impeding precise DNA synthesis. The cancer cells will die if they cannot repair the damaged DNA or the damage is too intense [97]. As shown in this study, OLO-2 inhibited ERCC1 protein expression in A549/CDDP cells. We speculated that the enhancement of CDDP induced DNA damage in the combination treatment may partly due to inhibition of ERCC1 by OLO-2.

OLO-2 also augmented the CDDP induced inhibition of the PI3K/AKT, MEK/ERK, NF-κB and STAT3 pathways in its parental A549 cells. This indicated that OLO-2

not only synergizes CDDP-induced inhibition of multiple signaling pathways in human multidrug-resistant lung adenocarcinoma cells but also can enhance CDDP-induced inhibition of multiple signaling pathways in drug-sensitive lung cancer cells.

As indicated in our study, OLO-2 inhibited TrxR expression and activity, and thus increasing ROS and DNA damage. The increased DNA damage will suppress PI3K/AKT and MEK/ERK pathways [62,63], as well as NF-κB and STAT3 pathways [67, 68]. OLO-2 could also inhibited P-gp expression and activity. It has been reported that P-gp expression is positively regulated by NF-κB [37], MEK/ERK [98] and PI3K/AKT [99] [100] signaling pathways. Therefore, OLO-2 most likely reduced P-gp mRNA level by inhibiting these three pathways. We speculate that these multiple action ways of OLO-2 might result from its multiple targeting characteristics. In order to address this issue, interrogating the direct targets of OLO-2 using bioinformatic and experimental methods, and elaborating the following biochemical reactions are warranted in the future work.

In conclusion, the present study demonstrates that OLO-2 could synergistically enhance CDDP-mediated apoptosis, lead to the activation of caspase-3 and ROS generation, cause DNA damage, and inhibit the ERK, STAT3, AKT and NF-κB signaling pathways and ERCC1 in A549/CDDP cells. Furthermore, OLO-2 inhibits

the expression of both TrxR and P-gp and their associated enzymatic activities, which leads to the downregulation of Trx and an augmentation of the above-mentioned effects. Further investigation on this composite may contribute to the development of novel cancer therapies associated with MDR in the future.

Funding

The present study was supported by the National Natural Science Foundation of China (grant nos. 81773179 and 81472355), the Key Project of Education Department and Finance Department and Teaching Guide committee of Hunan province (grant no. 15A141), and Provincial Natural Science Foundation of Hunan (2016JJ2172).

Ethics approval and consent to participate

Not applicable.

Patient consent for publication

Not applicable.

Competing interests

The authors declare that they have no competing interests.

References

[1] A. Jemal, F. Bray, M.M. Center, J. Ferlay, E. Ward, D. Forman, Global cancer statistics, CA Cancer J Clin 61(2) (2011) 69-90.

[2] R. Siegel, E. Ward, O. Brawley, A. Jemal, Cancer statistics, 2011: the impact of eliminating socioeconomic and racial disparities on premature cancer deaths, CA Cancer J Clin 61(4) (2011) 212-36.

[3] R. Siegel, D. Naishadham, A. Jemal, Cancer statistics, 2012, CA Cancer J Clin 62(1) (2012) 10-29.

[4] S.S. Devesa, F. Bray, A.P. Vizcaino, D.M. Parkin, International lung cancer trends by histologic type: male:female differences diminishing and adenocarcinoma rates rising, Int J Cancer 117(2) (2005) 294-9.

[5] R.D. Baird, S.B. Kaye, Drug resistance reversal--are we getting closer?, Eur J Cancer 39(17) (2003) 2450-61.

[6] R.W. Johnstone, A.A. Ruefli, M.J. Smyth, Multiple physiological functions for multidrug transporter P-glycoprotein?, Trends Biochem Sci 25(1) (2000) 1-6.

[7] X. Yang, K. Liu, P-gp Inhibition-Based Strategies for Modulating Pharmacokinetics of Anticancer Drugs: An Update, Curr Drug Metab 17(8) (2016) 806-826.

[8] G. Ondieki, M. Nyagblordzro, S. Kikete, R. Liang, L. Wang, X. He, Cytochrome P450 and P-Glycoprotein-Mediated Interactions Involving African Herbs Indicated for Common Noncommunicable Diseases, Evid Based Complement Alternat Med 2017 (2017) 2582463.

[9] P.D. Eckford, F.J. Sharom, ABC efflux pump-based resistance to chemotherapy drugs, Chem Rev 109(7) (2009) 2989-3011.

[10] D. Mustacich, G. Powis, Thioredoxin reductase, Biochem J 346 Pt 1 (2000) 1-8.

[11] E.S. Arner, A. Holmgren, Physiological functions of thioredoxin and thioredoxin reductase, Eur J Biochem 267(20) (2000) 6102-9.

[12] E.M. Hanschmann, J.R. Godoy, C. Berndt, C. Hudemann, C.H. Lillig, Thioredoxins, glutaredoxins, and peroxiredoxins--molecular mechanisms and health significance: from cofactors to antioxidants to redox signaling, Antioxid Redox Signal 19(13) (2013) 1539-605.

[13] S. Gromer, S. Urig, K. Becker, The thioredoxin system--from science to clinic, Med Res Rev 24(1) (2004) 40-89.

[14] M.P. Rigobello, V. Gandin, A. Folda, A.K. Rundlof, A.P. Fernandes, A. Bindoli, C. Marzano, M. Bjornstedt, Treatment of human cancer cells with selenite or tellurite in combination with auranofin enhances cell death due to redox shift, Free Radic Biol Med 47(6) (2009) 710-21.

[15] E.S. Arner, A. Holmgren, The thioredoxin system in cancer, Semin Cancer Biol 16(6) (2006) 420-6.

[16] K.F. Tonissen, G. Di Trapani, Thioredoxin system inhibitors as mediators of apoptosis for cancer therapy, Mol Nutr Food Res 53(1) (2009) 87-103.

[17] M. Benhar, I.L. Shytaj, J.S. Stamler, A. Savarino, Dual targeting of the thioredoxin and glutathione systems in cancer and HIV, J Clin Invest 126(5) (2016) 1630-9.

[18] M. Berggren, A. Gallegos, J.R. Gasdaska, P.Y. Gasdaska, J. Warneke, G. Powis, Thioredoxin and thioredoxin reductase gene expression in human tumors and cell lines, and the effects of serum stimulation and hypoxia, Anticancer Res 16(6B) (1996) 3459-66.

[19] D.T. Lincoln, E.M. Ali Emadi, K.F. Tonissen, F.M. Clarke, The thioredoxin-thioredoxin reductase

system: over-expression in human cancer, Anticancer Res 23(3B) (2003) 2425-33.
[20] L. Shao, M.B. Diccianni, T. Tanaka, R. Gribi, A.L. Yu, J.D. Pullen, B.M. Camitta, J. Yu, Thioredoxin expression in primary T-cell acute lymphoblastic leukemia and its therapeutic implication, Cancer Res 61(19) (2001) 7333-8.
[21] A. Yokomizo, M. Ono, H. Nanri, Y. Makino, T. Ohga, M. Wada, T. Okamoto, J. Yodoi, M. Kuwano, K. Kohno, Cellular levels of thioredoxin associated with drug sensitivity to cisplatin, mitomycin C, doxorubicin, and etoposide, Cancer Res 55(19) (1995) 4293-6.
[22] S.J. Kim, Y. Miyoshi, T. Taguchi, Y. Tamaki, H. Nakamura, J. Yodoi, K. Kato, S. Noguchi, High thioredoxin expression is associated with resistance to docetaxel in primary breast cancer, Clin Cancer Res 11(23) (2005) 8425-30.
[23] Y. Ai, B. Zhu, C. Ren, F. Kang, J. Li, Z. Huang, Y. Lai, S. Peng, K. Ding, J. Tian, Y. Zhang, Discovery of New Monocarbonyl Ligustrazine-Curcumin Hybrids for Intervention of Drug-Sensitive and Drug-Resistant Lung Cancer, J Med Chem 59(5) (2016) 1747-60.
[24] G. Chu, Cellular responses to cisplatin. The roles of DNA-binding proteins and DNA repair, J Biol Chem 269(2) (1994) 787-90.
[25] S. Yu, X. Qin, T. Chen, L. Zhou, X. Xu, J. Feng, MicroRNA-106b-5p regulates cisplatin chemosensitivity by targeting polycystic kidney disease-2 in non-small-cell lung cancer, Anticancer Drugs 28(8) (2017) 852-860.
[26] A.J. Chou, R. Gorlick, Chemotherapy resistance in osteosarcoma: current challenges and future directions, Expert Rev Anticancer Ther 6(7) (2006) 1075-85.
[27] A.K. Larsen, A.E. Escargueil, A. Skladanowski, Resistance mechanisms associated with altered intracellular distribution of anticancer agents, Pharmacol Ther 85(3) (2000) 217-29.
[28] Y. Li, F. Ahmed, S. Ali, P.A. Philip, O. Kucuk, F.H. Sarkar, Inactivation of nuclear factor kappaB by soy isoflavone genistein contributes to increased apoptosis induced by chemotherapeutic agents in human cancer cells, Cancer Res 65(15) (2005) 6934-42.
[29] T. Gong, L. Cui, H. Wang, H. Wang, N. Han, Knockdown of KLF5 suppresses hypoxia-induced resistance to cisplatin in NSCLC cells by regulating HIF-1alpha-dependent glycolysis through inactivation of the PI3K/Akt/mTOR pathway, J Transl Med 16(1) (2018) 164.
[30] Z.L. Liu, B.J. Jin, C.G. Cheng, F.X. Zhang, S.W. Wang, Y. Wang, B. Wu, Apatinib resensitizes cisplatin-resistant non-small cell lung carcinoma A549 cell through reversing multidrug resistance and suppressing ERK signaling pathway, Eur Rev Med Pharmacol Sci 21(23) (2017) 5370-5377.
[31] P. Jin, Y. Liu, R. Wang, STAT3 regulated miR-216a promotes ovarian cancer proliferation and cisplatin resistance, Biosci Rep 38(4) (2018).
[32] G. Rathnasamy, V. Sivakumar, P. Rangarajan, W.S. Foulds, E.A. Ling, C. Kaur, NF-kappaB-mediated nitric oxide production and activation of caspase-3 cause retinal ganglion cell death in the hypoxic neonatal retina, Invest Ophthalmol Vis Sci 55(9) (2014) 5878-89.
[33] Z. Bognar, K. Fekete, C. Antus, E. Hocsak, R. Bognar, A. Tapodi, A. Boronkai, N. Farkas, F. Gallyas, Jr., B. Sumegi, A. Szanto, Desethylamiodarone-A metabolite of amiodarone-Induces apoptosis on T24 human bladder cancer cells via multiple pathways, PLoS One 12(12) (2017) e0189470.
[34] J.Y. Song, C.S. Kim, J.H. Lee, S.J. Jang, S.W. Lee, J.J. Hwang, C. Lim, G. Lee, J. Seo, S.Y. Cho, J. Choi, Dual inhibition of MEK1/2 and EGFR synergistically induces caspase-3-dependent apoptosis in EGFR inhibitor-resistant lung cancer cells via BIM upregulation, Invest New Drugs 31(6) (2013) 1458-65.
[35] S.H. Kang, S.J. Jeong, S.H. Kim, J.H. Kim, J.H. Jung, W. Koh, J.H. Kim, D.K. Kim, C.Y. Chen, S.H. Kim, Icariside II induces apoptosis in U937 acute myeloid leukemia cells: role of inactivation of

STAT3-related signaling, PLoS One 7(4) (2012) e28706.
[36] X. Li, P. Mu, H. Qiao, J. Wen, Y. Deng, JNK-AKT-NF-kappaB controls P-glycoprotein expression to attenuate the cytotoxicity of deoxynivalenol in mammalian cells, Biochem Pharmacol 156 (2018) 120-134.
[37] Y. Xin, F. Yin, S. Qi, L. Shen, Y. Xu, L. Luo, L. Lan, Z. Yin, Parthenolide reverses doxorubicin resistance in human lung carcinoma A549 cells by attenuating NF-kappaB activation and HSP70 up-regulation, Toxicol Lett 221(2) (2013) 73-82.
[38] Y.Y. Chen, Y.J. Lin, W.T. Huang, C.C. Hung, H.Y. Lin, Y.C. Tu, D.M. Liu, S.J. Lan, M.J. Sheu, Demethoxycurcumin-Loaded Chitosan Nanoparticle Downregulates DNA Repair Pathway to Improve Cisplatin-Induced Apoptosis in Non-Small Cell Lung Cancer, Molecules 23(12) (2018).
[39] M.B. Sporn, K.T. Liby, M.M. Yore, L. Fu, J.M. Lopchuk, G.W. Gribble, New synthetic triterpenoids: potent agents for prevention and treatment of tissue injury caused by inflammatory and oxidative stress, J Nat Prod 74(3) (2011) 537-45.
[40] M.K. Shanmugam, X. Dai, A.P. Kumar, B.K. Tan, G. Sethi, A. Bishayee, Oleanolic acid and its synthetic derivatives for the prevention and therapy of cancer: preclinical and clinical evidence, Cancer Lett 346(2) (2014) 206-16.
[41] T.A. Stadheim, N. Suh, N. Ganju, M.B. Sporn, A. Eastman, The novel triterpenoid 2-cyano-3,12-dioxooleana-1,9-dien-28-oic acid (CDDO) potently enhances apoptosis induced by tumor necrosis factor in human leukemia cells, J Biol Chem 277(19) (2002) 16448-55.
[42] L. Gao, Y. Wang, Z. Xu, X. Li, J. Wu, S. Liu, P. Chu, Z. Sun, B. Sun, Y. Lin, J. Peng, G. Han, S. Wang, Z. Tang, SZC017, a novel oleanolic acid derivative, induces apoptosis and autophagy in human breast cancer cells, Apoptosis 20(12) (2015) 1636-50.
[43] F. Braga, D. Ayres-Saraiva, C.R. Gattass, M.A.M. Capella, Oleanolic acid inhibits the activity of the multidrug resistance protein ABCC1 (MRP1) but not of the ABCB1 (P-glycoprotein): Possible use in cancer chemotherapy, Cancer Letters 248(1) (2007) 147-152.
[44] Z. Zhang, C. Zhang, Y. Ding, Q. Zhao, L. Yang, J. Ling, L. Liu, H. Ji, Y. Zhang, The activation of p38 and JNK by ROS, contribute to OLO-2-mediated intrinsic apoptosis in human hepatocellular carcinoma cells, Food Chem Toxicol 63 (2014) 38-47.
[45] Y. Ding, Z. Huang, J. Yin, Y. Lai, S. Zhang, Z. Zhang, L. Fang, S. Peng, Y. Zhang, DDQ-promoted dehydrogenation from natural rigid polycyclic acids or flexible alkyl acids to generate lactones by a radical ion mechanism, Chem Commun (Camb) 47(33) (2011) 9495-7.
[46] J.G. Wang, X.X. Zheng, G.Y. Zeng, Y.J. Zhou, H. Yuan, Purified vitexin compound 1 induces apoptosis through activation of FOXO3a in hepatocellular carcinoma, Oncol Rep 31(1) (2014) 488-96.
[47] H. Li, J. Xu, X. Wang, G. Yuan, Protective effect of ginsenoside Rg1 on lidocaine-induced apoptosis, Mol Med Rep 9(2) (2014) 395-400.
[48] W. Jia, X. Jiang, W. Liu, L. Wang, B. Zhu, H. Zhu, X. Liu, M. Zhong, D. Xie, W. Huang, W. Jia, S. Li, X. Liu, X. Zuo, D. Cheng, J. Dai, C. Ren, Effects of three-dimensional collagen scaffolds on the expression profiles and biological functions of glioma cells, Int J Oncol (2018).
[49] H. Liu, C. Ren, B. Zhu, L. Wang, W. Liu, J. Shi, J. Lin, X. Xia, F. Zeng, J. Chen, X. Jiang, High-Efficient Transfection of Human Embryonic Stem Cells by Single-Cell Plating and Starvation, Stem Cells Dev 25(6) (2016) 477-91.
[50] W. Liu, X. Liu, L. Wang, B. Zhu, C. Zhang, W. Jia, H. Zhu, X. Liu, M. Zhong, D. Xie, Y. Liu, S. Li, J. Shi, J. Lin, X. Xia, X. Jiang, C. Ren, PLCD3, a flotillin2-interacting protein, is involved in proliferation, migration and invasion of nasopharyngeal carcinoma cells, Oncol Rep 39(1) (2018) 45-52.

[51] Y. Mi, C. Xiao, Q. Du, W. Wu, G. Qi, X. Liu, Momordin Ic couples apoptosis with autophagy in human hepatoblastoma cancer cells by reactive oxygen species (ROS)-mediated PI3K/Akt and MAPK signaling pathways, Free Radic Biol Med 90 (2016) 230-42.

[52] Q. Xie, G. Lan, Y. Zhou, J. Huang, Y. Liang, W. Zheng, X. Fu, C. Fan, T. Chen, Strategy to enhance the anticancer efficacy of X-ray radiotherapy in melanoma cells by platinum complexes, the role of ROS-mediated signaling pathways, Cancer Lett 354(1) (2014) 58-67.

[53] A. Charruyer, C. Jean, A. Colomba, J.P. Jaffrezou, A. Quillet-Mary, G. Laurent, C. Bezombes, PKCzeta protects against UV-C-induced apoptosis by inhibiting acid sphingomyelinase-dependent ceramide production, Biochem J 405(1) (2007) 77-83.

[54] H. Wang, S. Bouzakoura, S. de Mey, H. Jiang, K. Law, I. Dufait, C. Corbet, V. Verovski, T. Gevaert, O. Feron, D. Van den Berge, G. Storme, M. De Ridder, Auranofin radiosensitizes tumor cells through targeting thioredoxin reductase and resulting overproduction of reactive oxygen species, Oncotarget 8(22) (2017) 35728-35742.

[55] H. Hwang-Bo, J.W. Jeong, M.H. Han, C. Park, S.H. Hong, G.Y. Kim, S.K. Moon, J. Cheong, W.J. Kim, Y.H. Yoo, Y.H. Choi, Auranofin, an inhibitor of thioredoxin reductase, induces apoptosis in hepatocellular carcinoma Hep3B cells by generation of reactive oxygen species, Gen Physiol Biophys 36(2) (2017) 117-128.

[56] J. Su, H. Lai, J. Chen, L. Li, Y.S. Wong, T. Chen, X. Li, Natural borneol, a monoterpenoid compound, potentiates selenocystine-induced apoptosis in human hepatocellular carcinoma cells by enhancement of cellular uptake and activation of ROS-mediated DNA damage, PLoS One 8(5) (2013) e63502.

[57] Y. Wang, H. Lu, D. Wang, S. Li, K. Sun, X. Wan, E.W. Taylor, J. Zhang, Inhibition of glutathione synthesis eliminates the adaptive response of ascitic hepatoma 22 cells to nedaplatin that targets thioredoxin reductase, Toxicol Appl Pharmacol 265(3) (2012) 342-50.

[58] H. Steinbrenner, H. Sies, Protection against reactive oxygen species by selenoproteins, Biochim Biophys Acta 1790(11) (2009) 1478-85.

[59] C.H. Yang, C. Wang, I. Ojima, S.B. Horwitz, Taxol Analogues Exhibit Differential Effects on Photoaffinity Labeling of beta-Tubulin and the Multidrug Resistance Associated P-Glycoprotein, J Nat Prod 81(3) (2018) 600-606.

[60] D. Steinbach, O. Legrand, ABC transporters and drug resistance in leukemia: was P-gp nothing but the first head of the Hydra?, Leukemia 21(6) (2007) 1172-6.

[61] J.E. Rubnitz, How I treat pediatric acute myeloid leukemia, Blood 119(25) (2012) 5980-8.

[62] N. Yu, Y. Xiong, C. Wang, Bu-Zhong-Yi-Qi Decoction, the Water Extract of Chinese Traditional Herbal Medicine, Enhances Cisplatin Cytotoxicity in A549/DDP Cells through Induction of Apoptosis and Autophagy, Biomed Res Int 2017 (2017) 3692797.

[63] K. Fadlalla, A. Watson, T. Yehualaeshet, T. Turner, T. Samuel, Ruta graveolens extract induces DNA damage pathways and blocks Akt activation to inhibit cancer cell proliferation and survival, Anticancer Res 31(1) (2011) 233-41.

[64] Y. Tian, Q. Xie, Y. Tian, Y. Liu, Z. Huang, C. Fan, B. Hou, D. Sun, K. Yao, T. Chen, Radioactive (1)(2)(5)I seed inhibits the cell growth, migration, and invasion of nasopharyngeal carcinoma by triggering DNA damage and inactivating VEGF-A/ERK signaling, PLoS One 8(9) (2013) e74038.

[65] S. Boldt, U.H. Weidle, W. Kolch, The role of MAPK pathways in the action of chemotherapeutic drugs, Carcinogenesis 23(11) (2002) 1831-8.

[66] M.A. Lawlor, D.R. Alessi, PKB/Akt: a key mediator of cell proliferation, survival and insulin

responses?, J Cell Sci 114(Pt 16) (2001) 2903-10.
[67] F.J. Bock, G. Krumschnabel, C. Manzl, L. Peintner, M.C. Tanzer, N. Hermann-Kleiter, G. Baier, L. Llacuna, J. Yelamos, A. Villunger, Loss of PIDD limits NF-kappaB activation and cytokine production but not cell survival or transformation after DNA damage, Cell Death Differ 20(4) (2013) 546-57.
[68] X. Shi, L. Wang, X. Li, J. Bai, J. Li, S. Li, Z. Wang, M. Zhou, Dihydroartemisinin induces autophagy-dependent death in human tongue squamous cell carcinoma cells through DNA double-strand break-mediated oxidative stress, Oncotarget 8(28) (2017) 45981-45993.
[69] B. Groner, V. von Manstein, Jak Stat signaling and cancer: Opportunities, benefits and side effects of targeted inhibition, Mol Cell Endocrinol (2017).
[70] K.J. Wu, J.M. Huang, H.J. Zhong, Z.Z. Dong, K. Vellaisamy, J.J. Lu, X.P. Chen, P. Chiu, D.W.J. Kwong, Q.B. Han, D.L. Ma, C.H. Leung, A natural product-like JAK2/STAT3 inhibitor induces apoptosis of malignant melanoma cells, PLoS One 12(6) (2017) e0177123.
[71] B.L. Probst, I. Trevino, L. McCauley, R. Bumeister, I. Dulubova, W.C. Wigley, D.A. Ferguson, RTA 408, A Novel Synthetic Triterpenoid with Broad Anticancer and Anti-Inflammatory Activity, PLoS One 10(4) (2015) e0122942.
[72] K. Kahlos, Y. Soini, M. Saily, P. Koistinen, S. Kakko, P. Paakko, A. Holmgren, V.L. Kinnula, Up-regulation of thioredoxin and thioredoxin reductase in human malignant pleural mesothelioma, Int J Cancer 95(3) (2001) 198-204.
[73] S. Wang, F. Liu, J. Zhu, P. Chen, H. Liu, Q. Liu, J. Han, DNA Repair Genes ERCC1 and BRCA1 Expression in Non-Small Cell Lung Cancer Chemotherapy Drug Resistance, Med Sci Monit 22 (2016) 1999-2005.
[74] D. Lan, L. Wang, R. He, J. Ma, Y. Bin, X. Chi, G. Chen, Z. Cai, Exogenous glutathione contributes to cisplatin resistance in lung cancer A549 cells, Am J Transl Res 10(5) (2018) 1295-1309.
[75] C. He, K. Lu, D. Liu, W. Lin, Nanoscale metal-organic frameworks for the co-delivery of cisplatin and pooled siRNAs to enhance therapeutic efficacy in drug-resistant ovarian cancer cells, J Am Chem Soc 136(14) (2014) 5181-4.
[76] M. Saitoh, H. Nishitoh, M. Fujii, K. Takeda, K. Tobiume, Y. Sawada, M. Kawabata, K. Miyazono, H. Ichijo, Mammalian thioredoxin is a direct inhibitor of apoptosis signal-regulating kinase (ASK) 1, EMBO J 17(9) (1998) 2596-606.
[77] C. Wang, H. Ye, L. Zhang, Y. Cheng, S. Xu, P. Zhang, Z. Zhang, J. Bai, F. Meng, L. Zhong, G. Shi, H. Li, Enhanced expression of ten-eleven translocation 1 reverses gemcitabine resistance in cholangiocarcinoma accompanied by a reduction in P-glycoprotein expression, Cancer Med (2019).
[78] J.A. McCubrey, L.S. Steelman, S.L. Abrams, J.T. Lee, F. Chang, F.E. Bertrand, P.M. Navolanic, D.M. Terrian, R.A. Franklin, A.B. D'Assoro, J.L. Salisbury, M.C. Mazzarino, F. Stivala, M. Libra, Roles of the RAF/MEK/ERK and PI3K/PTEN/AKT pathways in malignant transformation and drug resistance, Adv Enzyme Regul 46 (2006) 249-79.
[79] J.A. McCubrey, L.S. Steelman, W.H. Chappell, S.L. Abrams, E.W. Wong, F. Chang, B. Lehmann, D.M. Terrian, M. Milella, A. Tafuri, F. Stivala, M. Libra, J. Basecke, C. Evangelisti, A.M. Martelli, R.A. Franklin, Roles of the Raf/MEK/ERK pathway in cell growth, malignant transformation and drug resistance, Biochim Biophys Acta 1773(8) (2007) 1263-84.
[80] H. Hu, C. Jiang, G. Li, J. Lu, PKB/AKT and ERK regulation of caspase-mediated apoptosis by methylseleninic acid in LNCaP prostate cancer cells, Carcinogenesis 26(8) (2005) 1374-81.
[81] L. Rosenberg, C.H. Yoon, G. Sharma, M.M. Bertagnolli, N.L. Cho, Sorafenib inhibits proliferation and invasion in desmoid-derived cells by targeting Ras/MEK/ERK and PI3K/Akt/mTOR pathways,

Carcinogenesis 39(5) (2018) 681-688.

[82] J. Renshaw, K.R. Taylor, R. Bishop, M. Valenti, A. De Haven Brandon, S. Gowan, S.A. Eccles, R.R. Ruddle, L.D. Johnson, F.I. Raynaud, J.L. Selfe, K. Thway, T. Pietsch, A.D. Pearson, J. Shipley, Dual blockade of the PI3K/AKT/mTOR (AZD8055) and RAS/MEK/ERK (AZD6244) pathways synergistically inhibits rhabdomyosarcoma cell growth in vitro and in vivo, Clin Cancer Res 19(21) (2013) 5940-51.

[83] T. Shimizu, A.W. Tolcher, K.P. Papadopoulos, M. Beeram, D.W. Rasco, L.S. Smith, S. Gunn, L. Smetzer, T.A. Mays, B. Kaiser, M.J. Wick, C. Alvarez, A. Cavazos, G.L. Mangold, A. Patnaik, The clinical effect of the dual-targeting strategy involving PI3K/AKT/mTOR and RAS/MEK/ERK pathways in patients with advanced cancer, Clin Cancer Res 18(8) (2012) 2316-25.

[84] X. Lin, X. Zhang, Q. Wang, J. Li, P. Zhang, M. Zhao, X. Li, Perifosine downregulates MDR1 gene expression and reverses multidrug-resistant phenotype by inhibiting PI3K/Akt/NF-kappaB signaling pathway in a human breast cancer cell line, Neoplasma 59(3) (2012) 248-56.

[85] J. Bosch-Barrera, B. Queralt, J.A. Menendez, Targeting STAT3 with silibinin to improve cancer therapeutics, Cancer Treat Rev 58 (2017) 61-69.

[86] Y. Suzuki-Karasaki, M. Suzuki-Karasaki, M. Uchida, T. Ochiai, Depolarization Controls TRAIL-Sensitization and Tumor-Selective Killing of Cancer Cells: Crosstalk with ROS, Front Oncol 4 (2014) 128.

[87] D. Zhou, L. Shao, D.R. Spitz, Reactive oxygen species in normal and tumor stem cells, Adv Cancer Res 122 (2014) 1-67.

[88] J.H. Cheng, A.M. Huang, T.C. Hour, S.C. Yang, Y.S. Pu, C.N. Lin, Antioxidant xanthone derivatives induce cell cycle arrest and apoptosis and enhance cell death induced by cisplatin in NTUB1 cells associated with ROS, Eur J Med Chem 46(4) (2011) 1222-31.

[89] I.L. Ho, K.L. Kuo, S.H. Liu, H.C. Chang, J.T. Hsieh, J.T. Wu, C.K. Chiang, W.C. Lin, Y.C. Tsai, C.T. Chou, C.H. Hsu, Y.S. Pu, C.S. Shi, K.H. Huang, MLN4924 Synergistically Enhances Cisplatin-induced Cytotoxicity via JNK and Bcl-xL Pathways in Human Urothelial Carcinoma, Sci Rep 5 (2015) 16948.

[90] T. Shono, P.J. Tofilon, T.S. Schaefer, D. Parikh, T.J. Liu, F.F. Lang, Apoptosis induced by adenovirus-mediated p53 gene transfer in human glioma correlates with site-specific phosphorylation, Cancer Res 62(4) (2002) 1069-76.

[91] T. Sasada, S. Iwata, N. Sato, Y. Kitaoka, K. Hirota, K. Nakamura, A. Nishiyama, Y. Taniguchi, A. Takabayashi, J. Yodoi, Redox control of resistance to cis-diamminedichloroplatinum (II) (CDDP): protective effect of human thioredoxin against CDDP-induced cytotoxicity, J Clin Invest 97(10) (1996) 2268-76.

[92] M. Yamada, A. Tomida, H. Yoshikawa, Y. Taketani, T. Tsuruo, Increased expression of thioredoxin/adult T-cell leukemia-derived factor in cisplatin-resistant human cancer cell lines, Clin Cancer Res 2(2) (1996) 427-32.

[93] M.Y. Kim SJ, Taguchi T, Tamaki Y, Nakamura H, Yodoi J, et al., High Thioredoxin Expression Is Associated with Resistance to Docetaxel in Primary Breast Cancer, Clin Cancer Res 11(23) (2005) 8425-8430.

[94] D.K. Das, N. Maulik, Conversion of death signal into survival signal by redox signaling, Biochemistry (Mosc) 69(1) (2004) 10-7.

[95] A.J. Freemerman, A. Gallegos, G. Powis, Nuclear factor kappaB transactivation is increased but is not involved in the proliferative effects of thioredoxin overexpression in MCF-7 breast cancer cells, Cancer Res 59(16) (1999) 4090-4.

[96] X. Ren, L. Zou, J. Lu, A. Holmgren, Selenocysteine in mammalian thioredoxin reductase and

application of ebselen as a therapeutic, Free Radic Biol Med (2018).
[97] L. Amable, Cisplatin resistance and opportunities for precision medicine, Pharmacol Res 106 (2016) 27-36.
[98] H. Zhang, H. Jiang, H. Zhang, J. Liu, X. Hu, L. Chen, Ribophorin II potentiates P-glycoprotein- and ABCG2-mediated multidrug resistance via activating ERK pathway in gastric cancer, Int J Biol Macromol 128 (2019) 574-582.
[99] Y. Li, Z. Zhai, H. Li, X. Wang, Y. Huang, X. Su, Guajadial reverses multidrug resistance by inhibiting ABC transporter expression and suppressing the PI3K/Akt pathway in drug-resistant breast cancer cells, Chem Biol Interact 305 (2019) 98-104.
[100] Q. Guo, F.J. Jing, H.J. Qu, W. Xu, B. Han, X.M. Xing, H.Y. Ji, F.B. Jing, Ubenimex Reverses MDR in Gastric Cancer Cells by Activating Caspase-3-Mediated Apoptosis and Suppressing the Expression of Membrane Transport Proteins, Biomed Res Int 2019 (2019) 4390839.

Figure 1. OLO-2 inhibits the viability of human lung cancer cells and human bronchial epithelial cell line HBE. (A) Structure of OLO-2. (B) Inhibition ratios of OLO-2 in human A549 and HBE cells. (C) Inhibition ratios of OLO-2 in human A549/CDDP and HBE cells. (D). Inhibition ratios of OLO-2 in human LTEP-a-2 and HBE cells. (E). Inhibition ratios of OLO-2 in human of SPC-A-1 and HBE cells. Data are representative of 3 independent experiments and all the controls were treated with the vehicle, DMSO (0.1%, v/v) alone. Differences were analyzed by a Student's t-test using SPSS version 18.0 statistical software (SPSS, Inc., Chicago, IL, USA). $^{*}P< 0.05$, $^{**}P< 0.01$ as compared to HBE cells. OLO-2, olean-28,13b-olide 2; A549/CDDP cells, the multidrug resistant human lung adenocarcinoma cell line.

Figure 2. OLO-2 inhibits TrxR expression at the protein and mRNA levels. (A) TrxR

expression in the A549/CDDP, A549 and HBE cells. (B) Quantification of TrxR expression in the A549/CDDP, A549, and HBE cells. (C) With an increasing concentration of OLO-2, the inhibition of TrxR and Trx proteins gradually became more pronounced. CDDO-ME exerted only a small influence on the protein expression levels of TrxR and Trx. (D) Fold changes of the TrxR and Trx protein expression levels. (E) OLO-2 inhibited TrxR mRNA expression, which was measured by RT-PCR. Data are representative of 3 independent experiments, and all the controls were treated with the vehicle, DMSO (0.1%, v/v) alone. Differences were analyzed by a Student's t-test using SPSS version 18.0 statistical software (SPSS, Inc., Chicago, IL, USA). For larger datasets involving >2 groups, one-way analysis of variance (ANOVA) with Bonferroni's multiple comparison tests was used. $^{*}P<0.05$, $^{**}P<0.01$, $^{***}P<0.001$ compared with the control. $^{\#}P<0.05$ vs. the CDDO-ME treatment group. OLO-2, olean-28,13b-olide 2; CDDP, cisplatin; TrxR, thioredoxin reductase; TRx, thioredoxin; PCR, polymerase chain reaction; CDDO(-ME), (methylated) 2-cyano-3,12-dioxoolean-1,9-dien-28-oic acid. A549/CDDP cells, the multidrug resistant human lung adenocarcinoma cell line.

Figure3. Influence of OLO-2 on the efflux of rh123 in A549/CDDP cells. (A) Expression of P-gp in the A549/CDDP and A549 cells. (B) Fold changes of P-gp expression in the A549/CDDP and A549 cells. (C) Accumulation of rh123 in the A549/CDDP cells was detected by flow cytometric assay. (D) With an increasing

concentration of OLO-2, the inhibition of P-pg proteins gradually became more pronounced. CDDO-ME exerted only a little influence on the protein expression levels of P-gp. (E) Fold changes of the P-gp protein expression levels. (F) OLO-2 inhibited P-gp mRNA expression, which was measured by RT-PCR. (G) OLO-2 and verapamil inhibited the efflux of rh123 in A549/CDDP cells, which was detected by fluorescence microscopy. Scale bar, 100 μm. Data are representative 3 three independent experiments and all the controls were treated with the vehicle, DMSO (0.1%, v/v) alone. Differences were analyzed by a Student's t-test using SPSS version 18.0 statistical software (SPSS, Inc., Chicago, IL, USA). For larger datasets involving >2 groups, one-way analysis of variance (ANOVA) with Bonferroni's multiple comparison tests was used. $^{***}P<0.001$ as compared with the control. OLO-2, olean-28,13b-olide 2; P-gp, P-glycoprotein; rh123, Rhodamine 123; CDDP, cisplatin.

Figure 4. OLO-2 synergistically enhances CDDP-mediated ROS accumulation and DNA damage. (A) OLO-2 enhanced CDDP-mediated ROS accumulation. A549/CDDP cells were treated with 1 μM OLO-2 for 1 h, and then treated with 20 μM CDDP for 2 h. ROS generation was subsequently measured using the fluorescence probe, DHE. (B) Pre-treatment with 10 mM NAC or GSH for 2 h clearly attenuated the inhibition resulting from combined treatment with 1 μM OLO-2 and 20 μM CDDP against A549/CDDP viability. (C) Treatment with 1 μM OLO-2 or 20 μM CDDP alone for 24 h induced DNA damage in the A549/CDDP cells, whereas combined treatment with 1 μM OLO-2 and 20 μM CDDP for 24 h significantly

enhanced DNA damage. Pre-treatment with 10 mM GSH for 2 h clearly reduced the combined effects on DNA damage. (D) Fold changes of H2A.X, Ser15-p53 and Ser20-p53 protein expression. Data are representative of 3 independent experiments and all the controls were treated with the vehicle, DMSO (0.1%, v/v) alone. Differences were analyzed by a Student's t-test using SPSS version 18.0 statistical software (SPSS, Inc., Chicago, IL, USA). For larger datasets involving >2 groups, one-way analysis of variance (ANOVA) with Bonferroni's multiple comparison tests was used. $^{*}P<0.05$, $^{**}P<0.01$, $^{***}P<0.001$ compared with the control. $^{\#}P<0.05$ vs. the OLO-2 alone or the CDDP alone group. $^{\&}P<0.05$ vs. the OLO-2 + CDDP group. OLO-2, olean-28,13b-olide 2 ; CDDP, cisplatin; ROS, reactive oxygen species; NAC, *N*-acetyl-L-cysteine (NAC); GSH, glutathione; DHE, dihydroethidium.

Figure 5. OLO-2 synergistically enhances the CDDP-induced inhibition of ERK, AKT, NF-κB and STAT3 pathways. (A) OLO-2 synergistically enhanced the CDDP-induced inactivation of ERK, p-ERK, AKT, p-AKT, NF-κB, p-NF-κB, STAT3 and p-STAT3. The protein expression levels were detected by western blot analysis. (B-I) Fold changes of the ERK, p-ERK, AKT, p-AKT, NF-κB, p-NF-κB, STAT3 and p-STAT3 protein expression levels. Data are representative of 3 independent experiments and all the controls were treated with the vehicle, DMSO (0.1%, v/v) alone. Differences were analyzed by a Student's t-test using SPSS version 18.0 statistical software (SPSS, Inc., Chicago, IL, USA). For larger datasets involving >2 groups, one-way analysis of variance (ANOVA) with Bonferroni's

multiple comparison tests was used. $^{**}P<0.01$, $^{***}P<0.001$ as compared with the control. $^{\#}P<0.05$ vs. CDDP alone group. $^{\&}P<0.05$ vs. OLO-2 alone group. OLO-2, olean-28,13b-olide 2; CDDP, cisplatin; ERK, extracellular-signal-activated kinase; NF-κB, nuclear factor-κB. p-NF-κB, Phospho-NF-κB p65 (Ser536); p-AKT, Phospho-Akt (Ser473); p-STAT3, Phospho-STAT3 (Ser727); p-ERK, Phospho-p44/42 MAPK (Erk1/2) (Thr202/Tyr204). U0126, an ERK inhibitor; LY294002, an upstream inhibitor of AKT; RTA-408, a specific NF-κB inhibitor; S3I-201, a STAT3 inhibitor.

Figure 6. Contribution of the ERK, AKT, NF-κB and STAT3 pathways to the inhibition of the viability of A549/CDDP cells induced by combined treatment CDDP and OLO-2. We used low concentrations of the inhibitors, so that the experiment could highlight the synergistic effects of OLO-2. (A and B) ERK, AKT, NF-κB and STAT3 inhibitors enhanced the inhibitory effects on the viability of A549/CDDP cells induced by combined treatment. The cells were pre-treated with 10 μM LY294002 (an upstream inhibitor of AKT), U0126 (an ERK inhibitor), 1 μM RTA 408 (a specific NF-κB inhibitor), or 60 μM S3I 201 (a STAT3 inhibitor) respectively for 2 h prior to the combined treatment with CDDP and OLO-2. Cell viability was detected by MTT assay. (C) LY294002 enhanced the inactivation of p-AKT induced by combined treatment. (D) U0126 enhanced the inactivation of p-ERK induced by combined treatment. (E) S3I-201 enhanced the inactivation of p-STAT3 induced by combined treatment. (F) RTA-408 enhanced the inactivation of p-NF-κB induced by combined

treatment. (G-J) Fold changes of inactivation of p-ERK, p-AKT, p-NF-κB and p-STAT3 induced by combined treatment. Data are representative of 3 independent experiments and all the controls were treated with the vehicle, DMSO (0.1%, v/v) alone. Differences were analyzed by a Student's t-test using SPSS version 18.0 statistical software (SPSS, Inc., Chicago, IL, USA). For larger datasets involving >2 groups, one-way analysis of variance (ANOVA) with Bonferroni's multiple comparison tests was used. $^{**}P<0.01$, $^{***}P<0.001$ as compared with the control. $^{\#}P<0.05$ vs. the OLO-2 0.5 μM + CDDP group. $^{\&}P<0.05$ vs. the OLO-2 1 μM + CDDP group. $^{@}P<0.05$ vs. OLO-2 + CDDP group.OLO-2, olean-28,13b-olide 2; CDDP, cisplatin; ERK, extracellular-signal-activated kinase; NF-κB, nuclear factor-κB. p-NF-κB, Phospho-NF-κB p65 (Ser536); p-AKT, Phospho-Akt (Ser473); p-STAT3, Phospho-STAT3 (Ser727); p-ERK, Phospho-p44/42 MAPK (Erk1/2) (Thr202/Tyr204). U0126, an ERK inhibitor; LY294002, an upstream inhibitor of AKT; RTA-408, a specific NF-κB inhibitor; S3I-201, a STAT3 inhibitor.

Figure 7. Inhibitors of PI3K/AKT, MEK/ERK, NFκB and STAT3 pathways could suppress CDDP resistance, detected by MTT assay. (A) LY294002 could reverse CDDP resistance. (B) U0126 could reverse CDDP resistance. (C) S3I 201 could reverse CDDP resistance. (D) RTA-408 could reverse CDDP resistance. Differences were analyzed by a Student's t-test using SPSS version 18.0 statistical software (SPSS, Inc., Chicago, IL, USA). For larger datasets involving >2 groups, one-way analysis of variance (ANOVA) with Bonferroni's multiple comparison tests was used. Data are

representative of 3 independent experiments and all the controls were treated with the vehicle, DMSO (0.1%, v/v) alone. *P<0.05 as compared with CDDP 20 μM group. U0126, an ERK inhibitor; LY294002, an upstream inhibitor of AKT; RTA-408, a specific NF-κB inhibitor; S3I-201, a STAT3 inhibitor. OLO-2, olean-28,13b-olide 2; CDDP, cisplatin; ERK, extracellular-signal-activated kinase; NF-κB, nuclear factor-κB.

Figure 8. OLO-2 synergistically enhances the CDDP-mediated apoptosis of A549/CDDP cells. (A) At concentrations of 2.5 and 5 μM, OLO-2, CDDO-ME and CDDP separately induced apoptosis. (B) Percentages of apoptotic cells induced by treatment with OLO-2, CDDO-ME or CDDP at concentrations of 2.5 and 5 μM. (C) CDDP at a concentration of 20 μM and combined treatment with various concentrations of OLO-2 induced apoptosis, which was inhibited by zVAD-fmk (a pan-caspase inhibitor). (D) Percentages of apoptotic cells induced by combined treatment with OLO-2 and CDDP. (E) A549/CDDP cells were treated with the vehicle (control), 20 μM CDDP (CDDP), 1 μM OLO-2 (OLO-2), 20 μM CDDP plus 1 μM OLO-2 (OLO-2 + CDDP), and zVAD-fmk combined with 20 μM CDDP and 1 μM OLO-2. The expression of caspase-3 and PARP was detected by western blot analysis. (F) Fold changes of caspase-3 and PARP protein expression. Differences were analyzed by a Student's t-test using SPSS version 18.0 statistical software (SPSS, Inc., Chicago, IL, USA). For larger datasets involving >2 groups, one-way analysis of

variance (ANOVA) with Bonferroni's multiple comparison tests was used. Data are representative of 3 independent experiments and all the controls were treated with the vehicle, DMSO (0.1%, v/v) alone. $^{*}P<0.05$, $^{**}P<0.01$, $^{***}P<0.001$ by ANOVA. $^{\#}P<0.05$ vs. the OLO-2 + CDDP group. OLO-2, olean-28,13b-olide 2; CDDP, cisplatin; PARP, poly (ADP-ribose) polymerase; CDDO(-ME), (methylated) 2-cyano-3,12-dioxoolean-1,9-dien-28-oic acid.

Figure 9. TrxR is a target of OLO-2 and is associated with the resistance of lung cancer cells to CDDP. (A) A549 and A549/CDDP cells were transfected with siRNA-TrxR for 48 h, and TrxR expression was detected by western blot analysis. The inhibitory rates of tumor cells were measured using an MTT assay. (B) A549 and A549/CDDP cells were transfected with pcDNA-3.1-TrxR for 48 h, and TrxR expression was detected by western blot analysis. The inhibitory rates of tumor cells were measured by MTT assay. (C) Detection of CDDP sensitivity before and after transfection. (D) Percentages of apoptotic cells induced by the treatments before and after transfection. Data are representative of 3 independent experiments and all the controls were treated with the vehicle, DMSO (0.1%, v/v) alone. $^{*}P<0.05$, $^{**}P<0.01$ compared with the control. OLO-2, olean-28,13b-olide 2; CDDP, cisplatin.

Figure 10. The TXNRD1 mRNA changes before and after the siRNA or plasmid transfections. (A) Realtime PCR detected the reduced TXNRD1 after transfection

with siRNA-TXNRD1 and non-targeting siRNA in A549 cells. (B) Realtime PCR detected the reduced TXNRD1 after transfection with siRNA-TXNRD1 and non-targeting siRNA in A549/CDDP cells. (C) Realtime PCR detected the increased TXNRD1 expression after transfection with pcDNA 3.1-TXNRD1 and pcDNA 3.1 in A549 cells. (D) Realtime PCR detected the increased TXNRD1 expression after transfection with pcDNA 3.1-TXNRD1 and pcDNA 3.1 in A549/CDDP cells. Differences were analyzed by a Student's t-test using SPSS version 18.0 statistical software (SPSS, Inc., Chicago, IL, USA). For larger datasets involving >2 groups, one-way analysis of variance (ANOVA) with Bonferroni's multiple comparison tests was used. Data are representative of 3 independent experiments and all the controls were treated with the vehicle, DMSO (0.1%, v/v) alone. $^{**}P<0.01$ compared with the controls.

Figure 11. OLO-2 inhibited ERCC1 in A549/DDP cells and the combination treatment suppressed PI3K/AKT, MEK/ERK, NFκB and STAT3 pathways in A549 cells. (A) With increasing concentrations of OLO-2, the inhibition of ERCC1 protein became more and more pronounced. (B) Fold changes of the ERCC1 protein expression levels. (C) The viability of A549 cells was inhibited by combination treatments of OLO-2 and CDDP, which was tested by MTT assay. (D) OLO-2 synergistically enhanced the CDDP-induced inactivation of p-ERK, AKT, p-AKT, p-NF-κB and p-STAT3 in A549 cells. The protein expression levels were detected by western blot analysis. (E-H) Fold changes of the p-ERK, p-AKT, p-NF-κB and

p-STAT3 protein expression levels. Data are representative of 3 independent experiments and all the controls were treated with the vehicle, DMSO (0.1%, v/v) alone. Differences were analyzed by a Student's t-test using SPSS version 18.0 statistical software (SPSS, Inc., Chicago, IL, USA). For larger datasets involving >2 groups, one-way analysis of variance (ANOVA) with Bonferroni's multiple comparison tests was used. $^{**}P<0.01$, $^{***}P<0.001$ as compared with the control. $^{\#}P<0.05$ vs. CDDP alone group. $^{\&}P<0.05$ vs. OLO-2 alone group. OLO-2, olean-28,13b-olide 2; CDDP, cisplatin; ERK, extracellular-signal-activated kinase; NF-κB, nuclear factor-κB. p-NF-κB, Phospho-NF-κB p65 (Ser536); p-AKT, Phospho-Akt (Ser473); p-STAT3, Phospho-STAT3 (Ser727); p-ERK, Phospho-p44/42 MAPK (Erk1/2) (Thr202/Tyr204).

Figure 12. Proposed mechanisms of OLO-2 reversed CDDP resistance and multidrug resistance through the inhibition of thioredoxin and multiple signaling pathways.

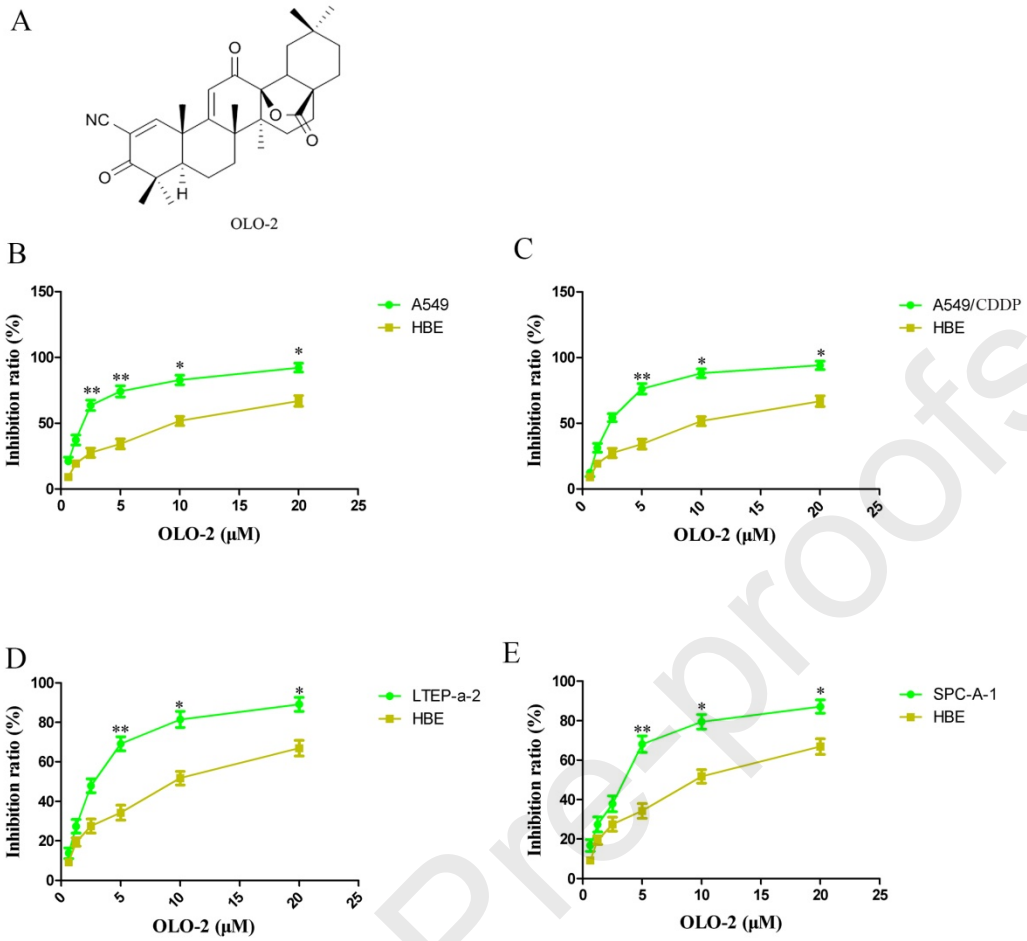

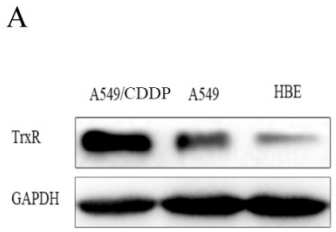

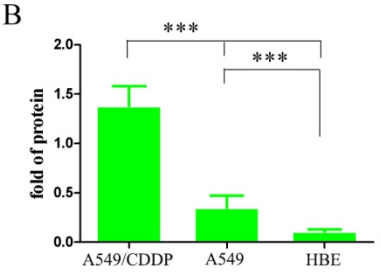

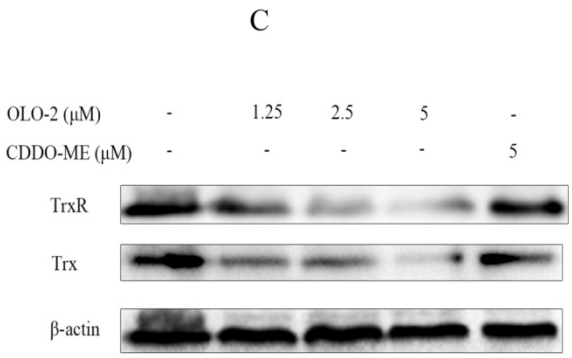

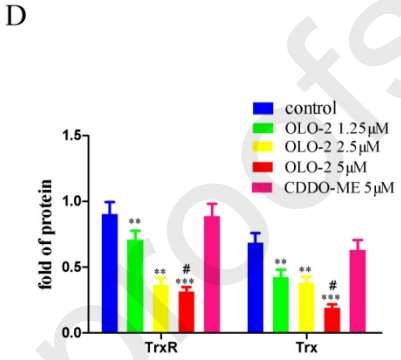

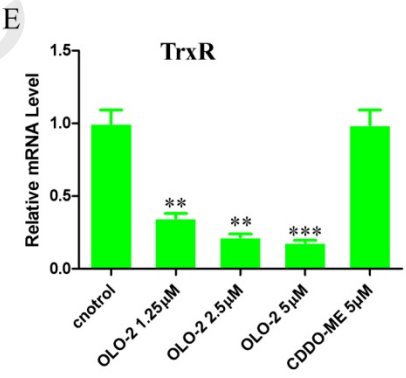

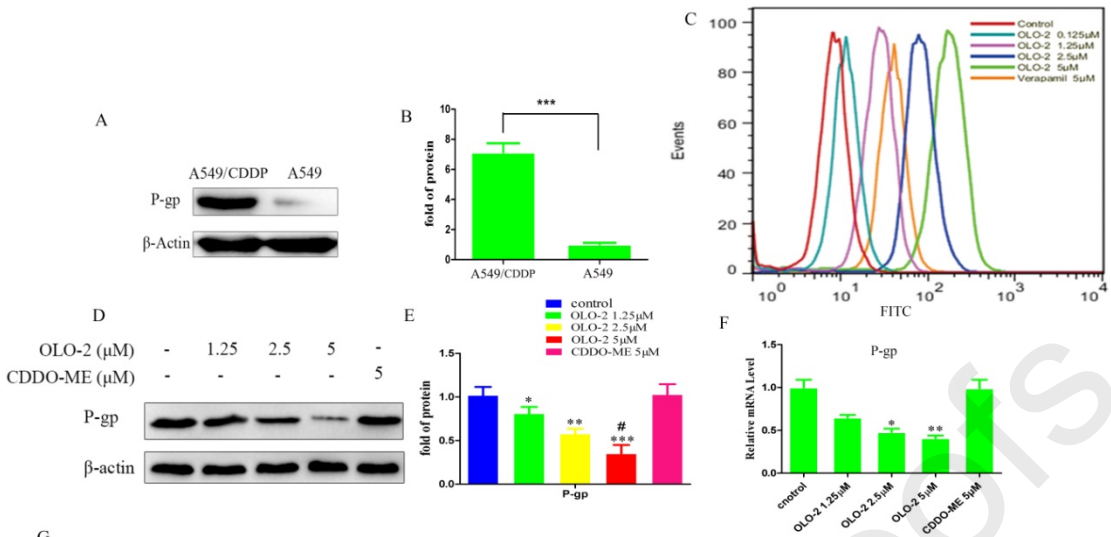
A
A549/CDDP
A549
P-gp
β-Actin
B
fold of protein
***
A549/CDDP
A549
C
Control
OLO-2 0.125μM
OLO-2 1.25μM
OLO-2 2.5μM
OLO-2 5μM
Verapamil 5μM
Events
FITC
D
OLO-2 (μM) - 1.25 2.5 5 -
CDDO-ME (μM) - - - - 5
P-gp
β-actin
E
control
OLO-2 1.25μM
OLO-2 2.5μM
OLO-2 5μM
CDDO-ME 5μM
fold of protein
P-gp
F
P-gp
Relative mRNA Level
cnotrol
OLO-2 1.25μM
OLO-2 2.5μM
OLO-2 5μM
CDDO-ME 5μM

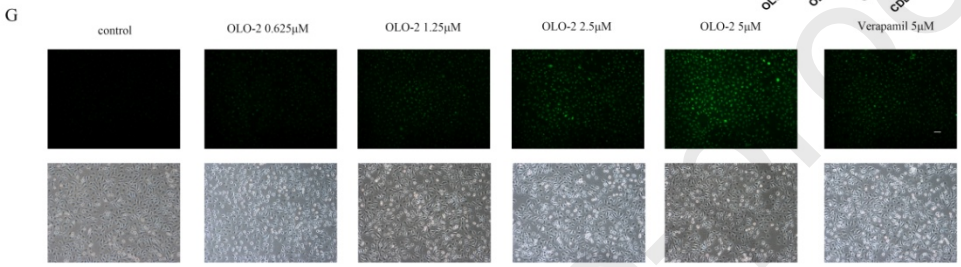
G
control
OLO-2 0.625μM
OLO-2 1.25μM
OLO-2 2.5μM
OLO-2 5μM
Verapamil 5μM

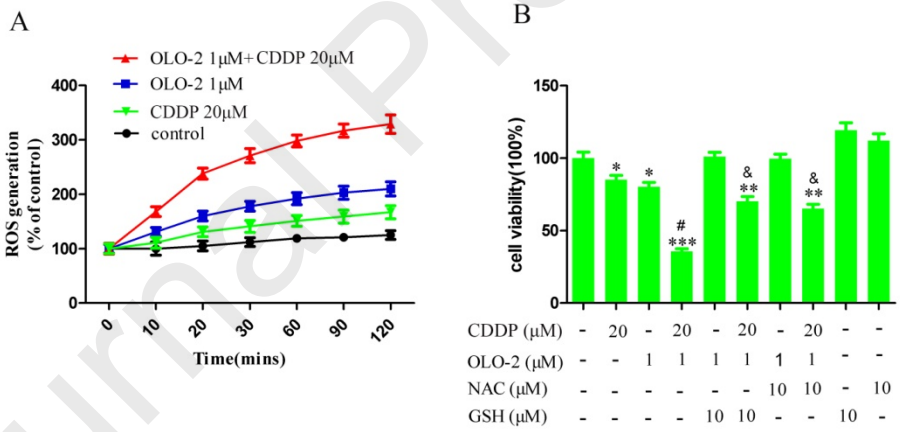
A
OLO-2 1μM+CDDP 20μM
OLO-2 1μM
CDDP 20μM
control
ROS generation (% of control)
Time(mins)
B
cell viability(100%)
CDDP (μM) - 20 - 20 - 20 - 20 - -
OLO-2 (μM) - - 1 1 1 1 1 1 - -
NAC (μM) - - - - - - 10 10 - 10
GSH (μM) - - - - 10 10 - - 10 -

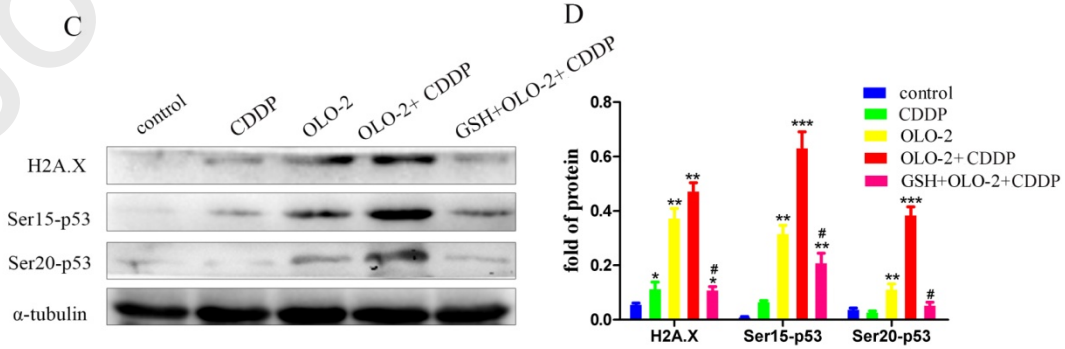
C
control
CDDP
OLO-2
OLO-2+ CDDP
GSH+OLO-2+CDDP
H2A.X
Ser15-p53
Ser20-p53
α-tubulin
D
control
CDDP
OLO-2
OLO-2+CDDP
GSH+OLO-2+CDDP
fold of protein
H2A.X
Ser15-p53
Ser20-p53

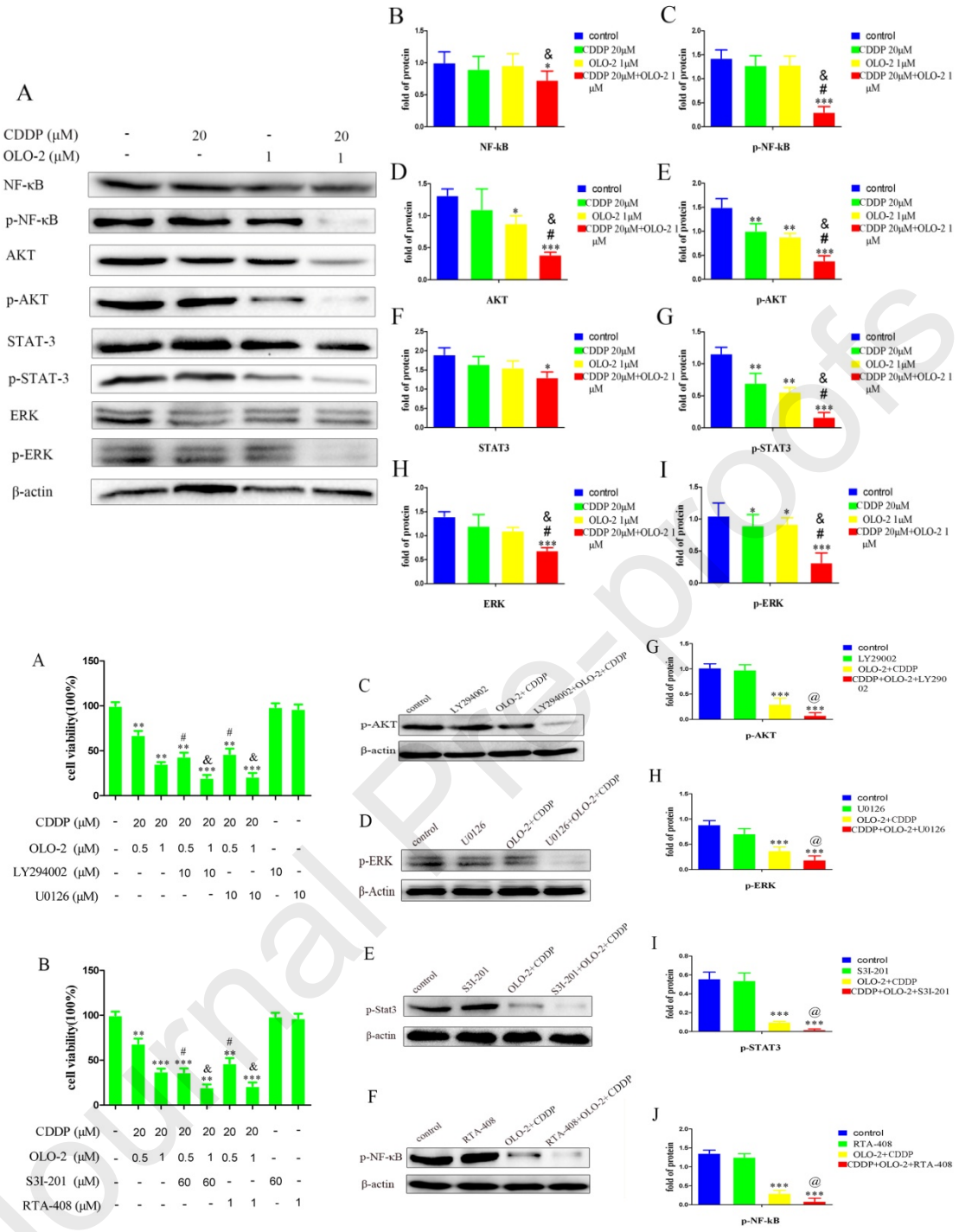

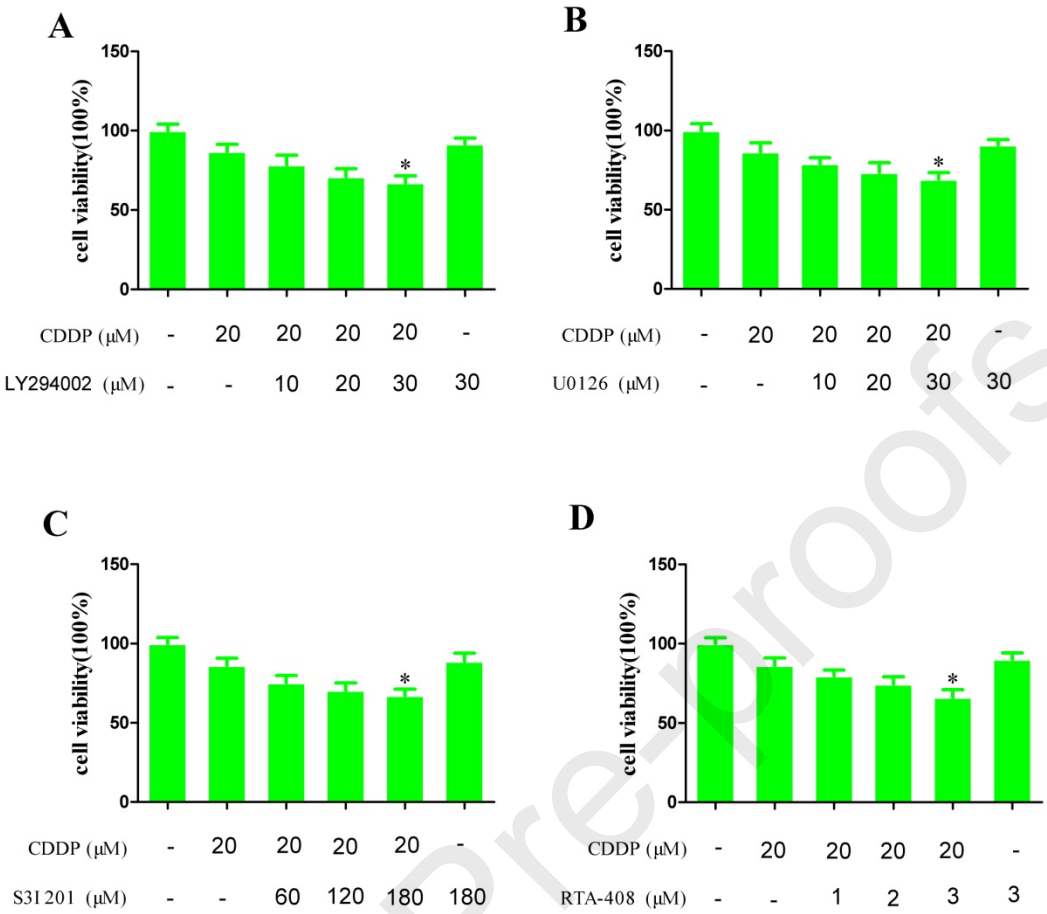

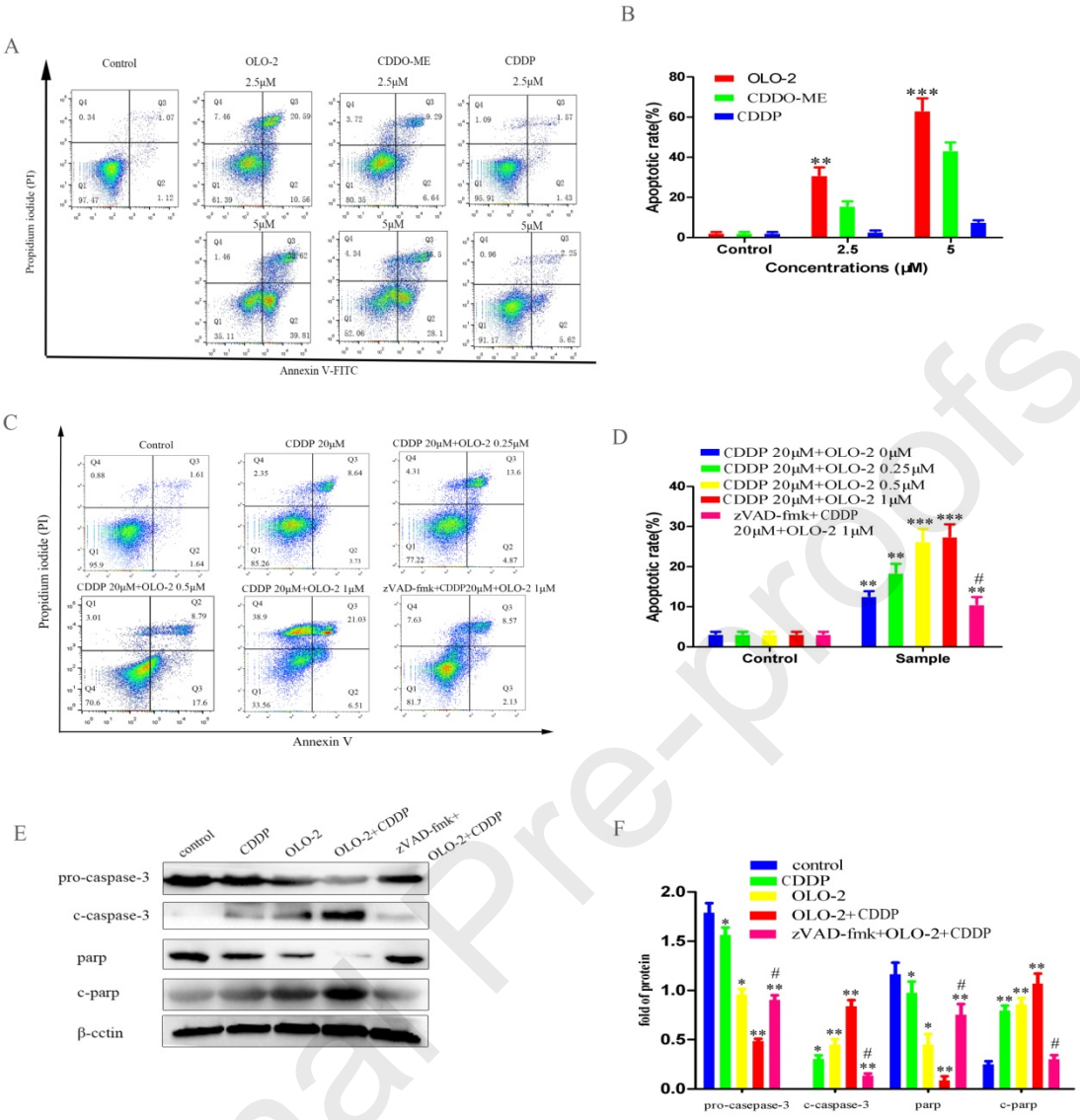

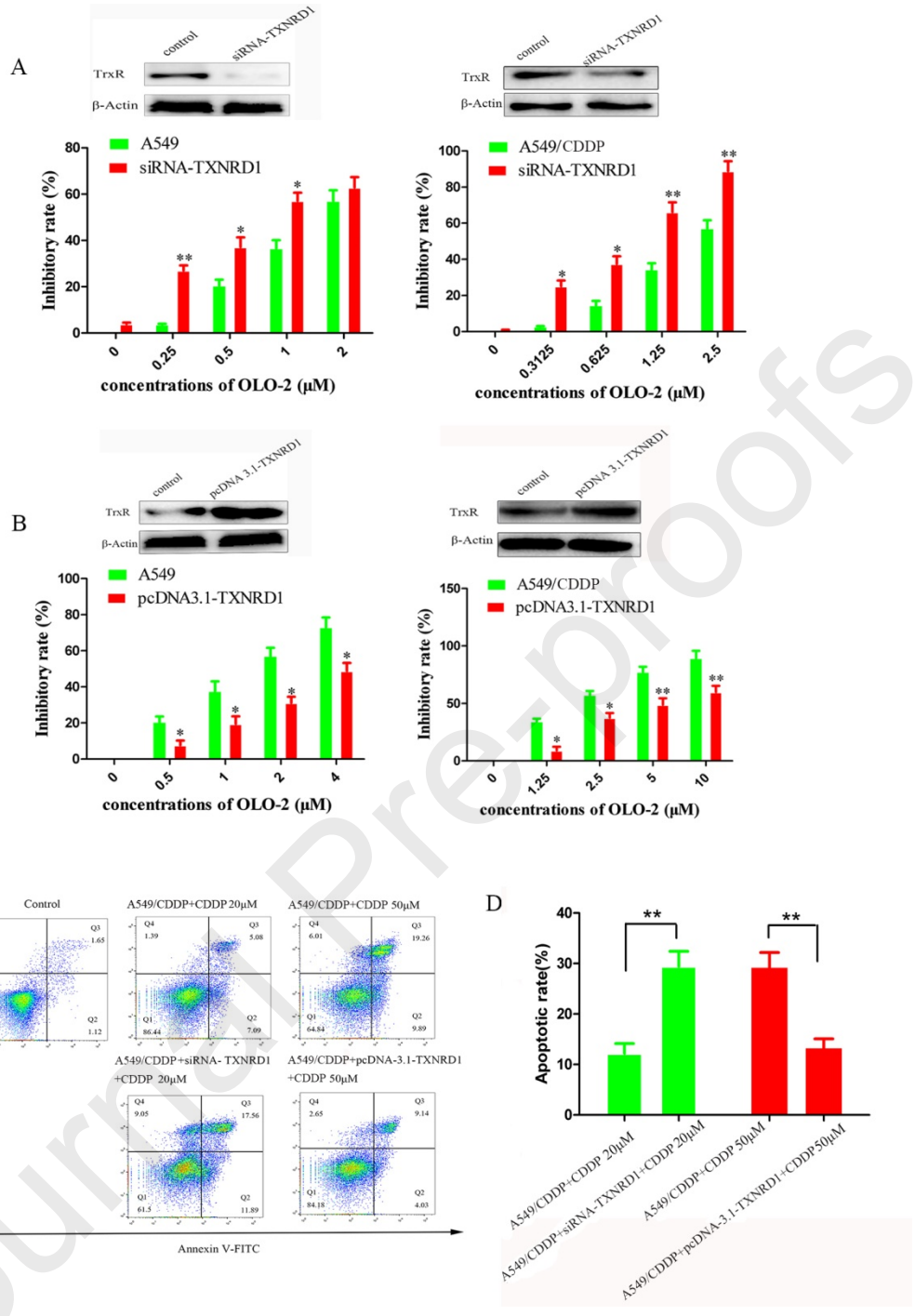
A
control
siRNA-TXNRD1
TrxR
β-Actin
A549
siRNA-TXNRD1
Inhibitory rate (%)
concentrations of OLO-2 (μM)
A549/CDDP
siRNA-TXNRD1
B
pcDNA 3.1-TXNRD1
pcDNA3.1-TXNRD1
C
Control
A549/CDDP+CDDP 20μM
A549/CDDP+CDDP 50μM
A549/CDDP+siRNA- TXNRD1 +CDDP 20μM
A549/CDDP+pcDNA-3.1-TXNRD1 +CDDP 50μM
Propidium iodide (PI)
Annexin V-FITC
D
Apoptotic rate(%)
A549/CDDP+CDDP 20μM
A549/CDDP+siRNA-TXNRD1+CDDP 20μM
A549/CDDP+CDDP 50μM
A549/CDDP+pcDNA-3.1-TXNRD1+CDDP 50μM

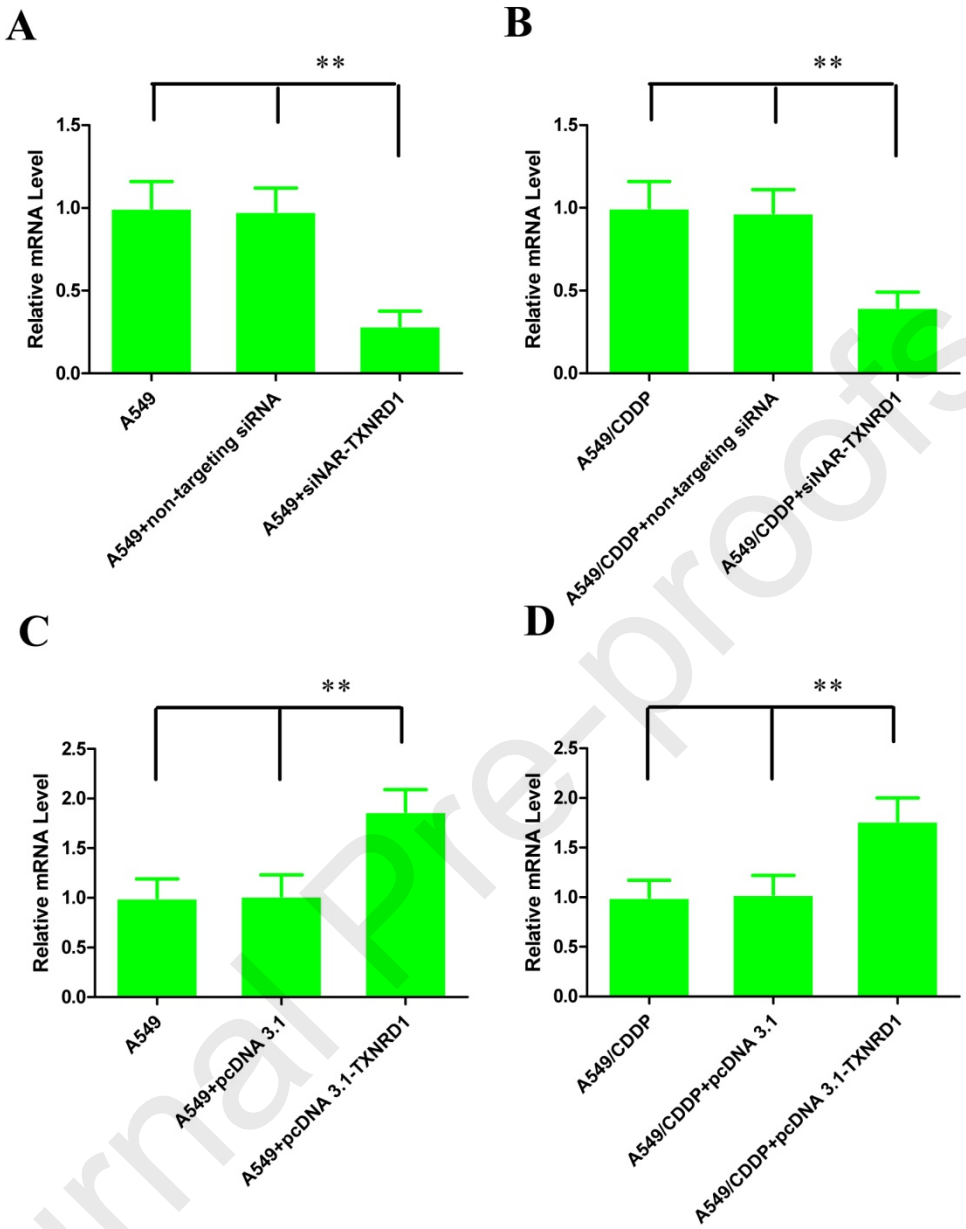

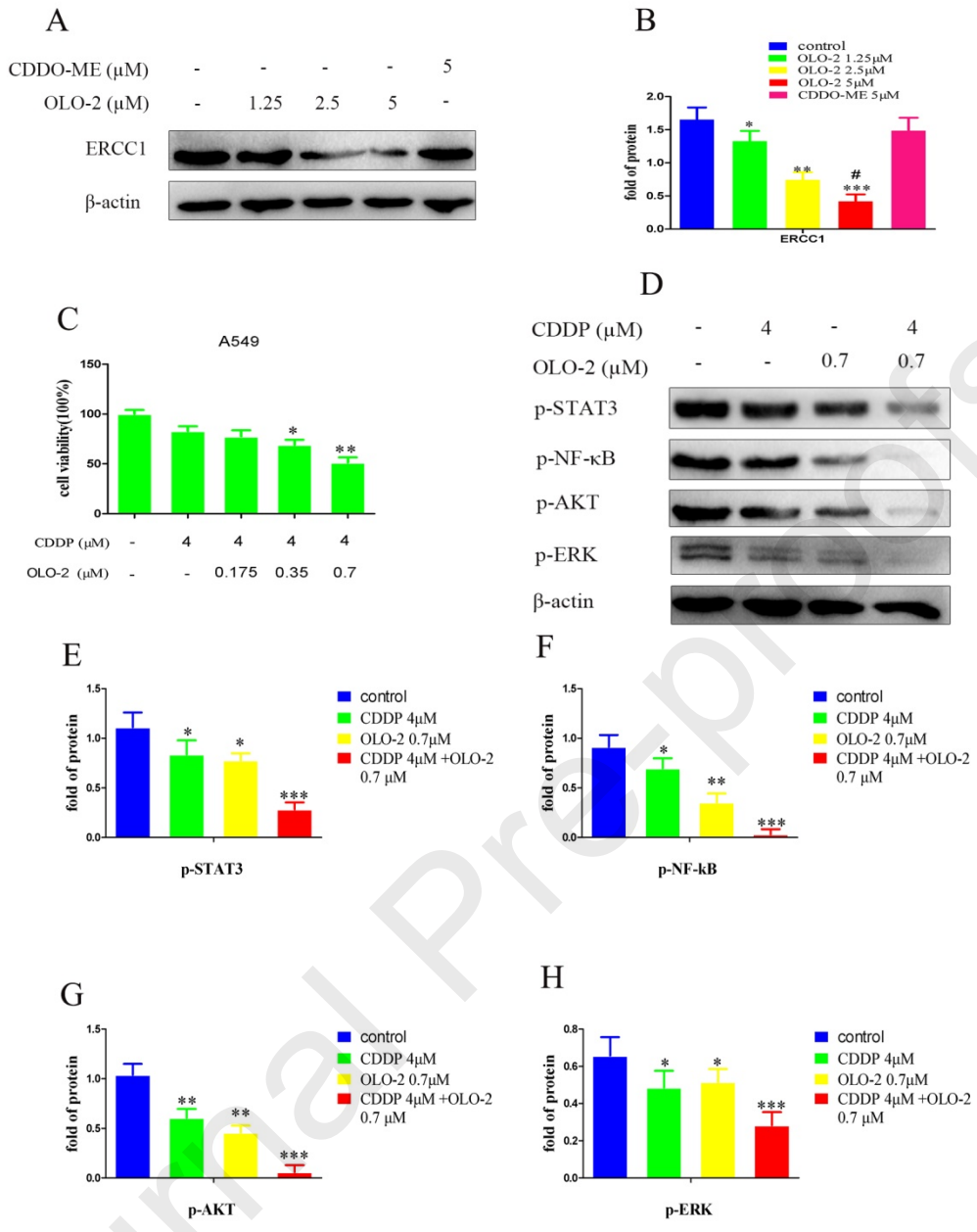

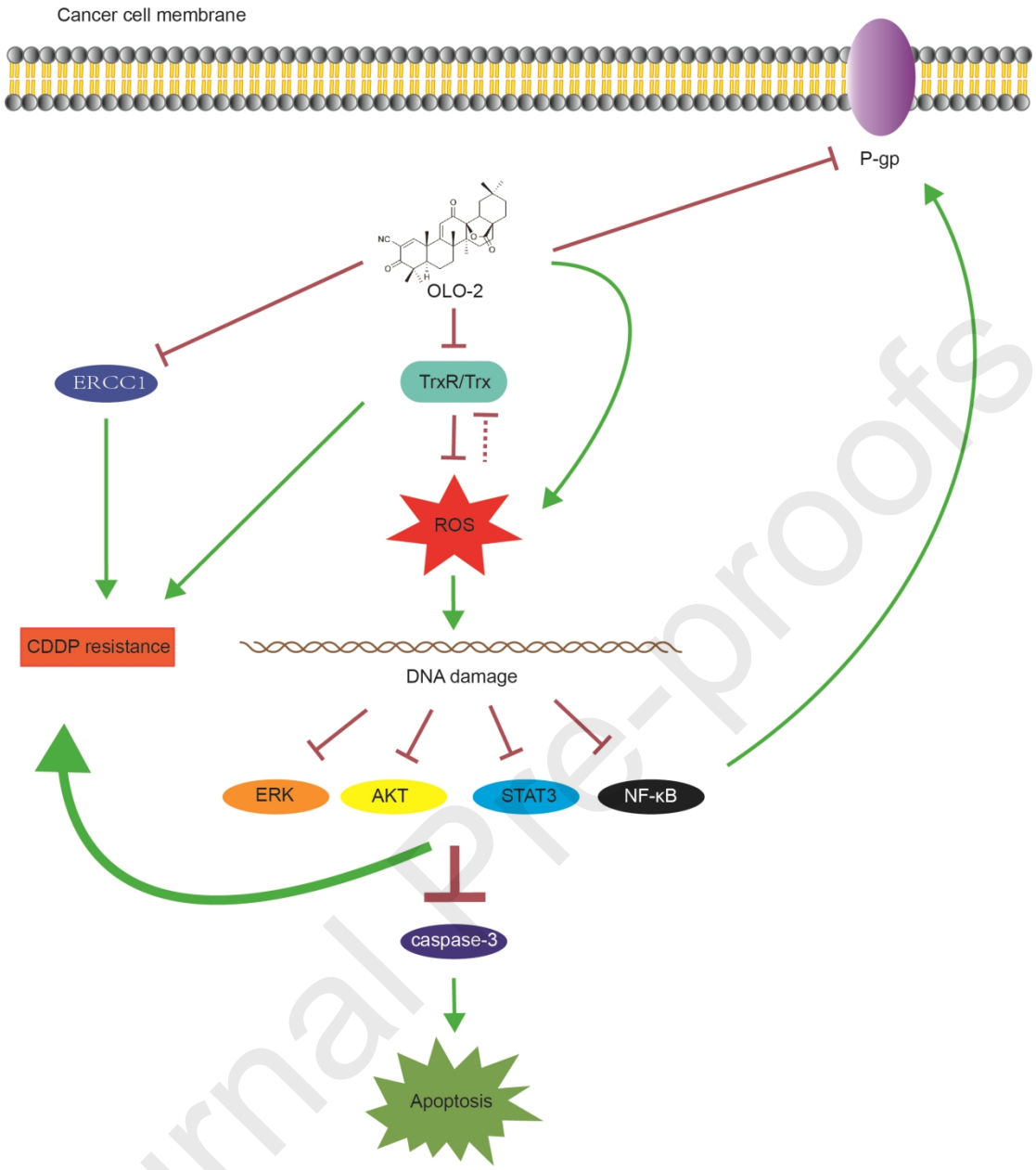

Table1

The IC_{50} values of OLO-2, CDDO-ME and CDDP in human lung adenocarcinoma cell lines and human bronchial epithelial cell line HBE.

compounds	$IC_{50}(\mu M)$[a]				
	A549	SPC-A-1	LTEP-a-2	A549/CDDP	HBE
OLO-2	1.96±0.41[b]	3.02±0.53[b]	2.80±0.66[b]	2.39±0.56[b]	9.07±1.26
CDDO-ME	2.51±0.37[b]	3.36±0.58[b]	2.71±0.47[b]	4.68±0.78[b]	8.16±0.68
CDDP	8.87±1.05[b]	16.17±1.45[b]	15.56±1.26[b]	48.67±3.07[b]	11.78±1.78

[a]The values of IC_{50} for each compound were calculated from three independent experiments and expressed as mean±SD. [b]$P< 0.05$ as compared to HBE cells.

Table 2.

OLO-2 inhibits TrxR activity in cell-free and cellular assays

		in cellular assay IC50(μM)[b]	
compounds	in cell-free assay IC50(μM)[a]	A549	A549/CDDP
OLO-2	0.95±0.11[c]	4.49±0.51[c]	3.14±0.32[c]
CDDO-ME	2.71±0.29	13.12±1.12	13.39±1.43

[a]The TrxR inhibitory activity of OLO-2 in cell-free assay was detected by DTNB assay as depicted in the **Materials and methods**. [b] Thioredoxin Reductase Assay Kit was used to detect the activity of TrxR. [c] $P<0.05$ as compared to CDDO-ME. Data are representatives of three independent experiments.

Table 3

compounds	concentration (μM)	luminescence (RLUs)[a]
untreated	0	512236±18356
verapamil	200	417889±17919*
Na_3VO_4	200	601760±14882**
OLO-2	40	587129±12772*

[a]Relative light units (RLUs) symbolize the levels of ATP in the samples, and are contrary to the activity of P-gp-ATPase. Data are representatives of three independent experiments. *$P< 0.05$, **$P< 0.01$ as compared to the untreated group.

Table4

The IC_{50} values of doxorubicin, vincristine and paclitaxel in human lung multidrug-resistant (A549/CDDP) non-small cell lung cancer cell lines and its parental A549 cell line.

compounds	IC_{50} (nM)[a]	
	A549	A549/CDDP
doxorubicin	11.38±1.41	577.89±65.12[b]
vincristine	141.76±7.64	2128.75±151.78[b]
paclitaxel	96.79±8.26	3787.92±261.82[b]

[a]The values of IC_{50} for each compound were calculated from three independent experiments and expressed as mean±SD. [b]$P< 0.001$ as compared to A549 cells.